



LUND UNIVERSITY

Addressing water scarcity in the Bolivian Altiplano for sustainable water management

Canedo Rosso, Claudia

2019

Document Version:

Publisher's PDF, also known as Version of record

[Link to publication](#)

Citation for published version (APA):

Canedo Rosso, C. (2019). *Addressing water scarcity in the Bolivian Altiplano for sustainable water management*. Water Resources Engineering, Lund University.

Total number of authors:

1

Creative Commons License:

CC BY

General rights

Unless other specific re-use rights are stated the following general rights apply:

Copyright and moral rights for the publications made accessible in the public portal are retained by the authors and/or other copyright owners and it is a condition of accessing publications that users recognise and abide by the legal requirements associated with these rights.

- Users may download and print one copy of any publication from the public portal for the purpose of private study or research.
- You may not further distribute the material or use it for any profit-making activity or commercial gain
- You may freely distribute the URL identifying the publication in the public portal

Read more about Creative commons licenses: <https://creativecommons.org/licenses/>

Take down policy

If you believe that this document breaches copyright please contact us providing details, and we will remove access to the work immediately and investigate your claim.

LUND UNIVERSITY

PO Box 117
221 00 Lund
+46 46-222 00 00

Addressing water scarcity in the Bolivian Altiplano for sustainable water management

CLAUDIA TERESA CANEDO ROSSO
FACULTY OF ENGINEERING | LUND UNIVERSITY



Addressing water scarcity in the Bolivian Altiplano for
sustainable water management

Addressing water scarcity in the Bolivian Altiplano for sustainable water management

Claudia Teresa Canedo Rosso



LUND
UNIVERSITY

DOCTORAL DISSERTATION

by due permission of the Faculty of Engineering, Lund University, Sweden.
To be defended at the Faculty of Engineering, V-building, John Ericssons väg 1,
Lund, room V:B on 13th June, 2019 at 10:15.

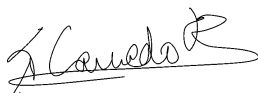
Faculty opponent

Prof. Dr. Josyane Ronchail
Université Paris Diderot

Organization LUND UNIVERSITY Division of Water Resources Engineering P.O. Box 118 SE-221 00 Lund Sweden		Document name Doctoral dissertation
		Date of issue 13th June 2019
Author Claudia Canedo-Rosso		Sponsoring organization Swedish International Development Cooperation Agency (SIDA)
Title and subtitle: Addressing water scarcity in the Bolivian Altiplano for sustainable water management		
Abstract Water scarcity is a consequence of complex interactions between water access and water use. In fact, the time period over which precipitation deficit accumulates is a determining factor for the occurrence of drought. Drought induces crop production losses and far-reaching societal effects. In the South American Altiplano, drought is a major hazard. Here, drought leads to food shortages, malnutrition, migration, loss of biodiversity, and local conflicts. In order to improve the drought resilience and develop mitigation and adaptation strategies, there is a need to study water scarcity episodes, and their drivers in the Bolivian Altiplano. Therefore, the main goal of this study was to address the Bolivian Altiplano water scarcity for sustainable water management. In the first instance, previous research on the subject was synthesized in a state of art with respect to climate and water resources. Secondly, analysis of precipitation variability, and its relation with climate phenomena were performed. It involved the analysis of the long-term austral summer precipitation variance at six locations in the Bolivian Altiplano. The precipitation variability was related to climate anomalies over the Pacific and Atlantic Ocean. The results show significant negative relationship between summer precipitation and climate phenomena in the studied region. Thirdly, a hydrological study to define the soil moisture characteristics was initiated in a river basin of the Bolivian Altiplano. It involved soil moisture estimations using soil water balance and satellite derived approaches. The estimated soil moisture was compared and validated with gauged soil moisture. The soil moisture estimations were used to define the impact of water scarcity in agricultural production. Finally, a drought risk analysis based on the association of precipitation and temperature variability with quinoa and potato yield was accomplished. For this, monthly satellite data of precipitation and temperature were validated with gauged data. The precipitation and temperature were related to agricultural production in the studied region. The normalized difference vegetation index was used to estimate the crop yield of the agricultural area. It was found that the variance of the agricultural production depends largely on the precipitation and temperature variance. The findings of this thesis provide insights in identifying strategies to improve the water management in the Bolivian Altiplano, mainly during water stress conditions. Moreover, the analyses enhance the knowledge for seasonal forecasting, drought disaster risk management, proactive planning, and mitigation policy measures in vulnerable regions of the Bolivian Altiplano.		
Key words: Hydrology, climatology, climate anomalies, climate modes, drought, water balance, ENSO, soil moisture, crop yield, remote sensing, Bolivian highlands, arid and semiarid regions.		
Classification system and/or index terms (if any)		
Supplementary bibliographical information		Language: English
ISSN and key title: 1101-9824		ISBN 978-91-7895-088-1 (print) ISBN 978-91-7895-089-8 (e-version)
Recipient's notes	Number of pages: 60	Price
	Security classification	

I, the undersigned, being the copyright owner of the abstract of the above-mentioned dissertation, hereby grant to all reference sources permission to publish and disseminate the abstract of the above-mentioned dissertation.

Signature



Date: 13th June 2019

Addressing water scarcity in the Bolivian Altiplano for sustainable water management

Claudia Teresa Canedo Rosso



LUND
UNIVERSITY

Cover photo by Jules Tusseau

Copyright 2019 Claudia Canedo-Rosso

Faculty of Engineering, Department of Building and Environmental Technology,
Division of Water Resources Engineering

Paper 1 © by MDPI

Paper 2 © by John Wiley & Sons, Inc.

Paper 3 © by the Authors (Manuscript unpublished)

Paper 4 © by the Authors (Manuscript under review for the Journal Natural
Hazards and Earth System Sciences)

ISBN printed version: 978-91-7895-088-1

ISBN e-version: 978-91-7895-089-8

ISSN: 1101-9824

Report N° 1077

Printed in Sweden by Media-Tryck, Lund University
Lund 2019



MADE IN SWEDEN 

Media-Tryck is an environmentally
certified and ISO 14001 certified
provider of printed material.
Read more about our environmental
work at www.mediatryck.lu.se

*To the indigenous people in the whole world, who
inspired me to take a stand on sustainability.*

Contents

List of figures	x
List of tables.....	x
Acknowledgements	xi
Popular summary	xii
Abbreviations	xiv
Papers	xvi
Appended papers	xvi
Author's contribution to appended papers.....	xvi
Other publications	xvii
Conference abstracts.....	xvii
Reports.....	xvii
Abstract	xviii
Resumen.....	xix
1. Introduction	1
2. Theoretical background.....	3
2.1. Climate variability.....	3
2.2. Water content in the soil.....	5
2.3. Drought	7
2.3.1. Drought concept and types	7
2.3.2. Global and local context of drought	9
3. Study area	11
4. Data.....	13
4.1. Precipitation and temperature.....	13
4.2. Other hydrological variables	14
4.3. Climate modes of variability	15
4.4. Crop yield and vegetation	16

5. Methods	19
5.1. Precipitation variability and its relation to climate phenomena	20
5.2. Soil moisture estimations	21
5.2.1. Soil water balance driven by precipitation	21
5.2.2. Soil water balance driven by satellite soil moisture	24
5.2.3. Calibration of the soil water balance model	25
5.2.4. Soil moisture variability relationship with agriculture	25
5.3. Drought risk assessment.....	26
5.3.1. Validation of satellite data using ground data	26
5.3.2. Crop yield simulation based on NDVI data.....	27
5.3.3. Regression of vegetation and climate variables.....	28
5.3.4. Crop yield relationship with ENSO.....	29
6. Results and discussion	31
6.1. Precipitation variability	32
6.1.1. Wavelet analysis.....	33
6.1.2. Band-pass filter reconstruction.....	36
6.2. Soil water estimations	36
6.2.1. Soil water balance calibration.....	37
6.2.2. Soil moisture estimations	37
6.3. Drought risk assessment.....	39
6.3.1. Validation of satellite imagery using gauged data.....	39
6.3.2. Regression of NDVI and climate variables	40
6.3.3. Relationship between ENSO and crop yield	42
7. Summary and conclusions	45
References	49

List of figures

Figure 1. The soil water balance.....	6
Figure 2. Drought occurrence and impacts.....	8
Figure 3. The Bolivian Altiplano in South America	12
Figure 4. Katari River sub-basin in the Bolivian Altiplano.....	15
Figure 5. Thesis framework.....	19
Figure 6. Boxplots of monthly precipitation	31
Figure 7. Mean monthly maximum and minimum temperature.....	32
Figure 8. Cross Wavelet Transform (CWT) for summer precipitation	33
Figure 9. Cross Wavelet Transform (CWT) for climate modes	34
Figure 10. Precipitation and soil moisture.....	37
Figure 11. Calibrated soil moisture estimations	38
Figure 12. Gauged and CHIRPS satellite-based precipitation.....	39
Figure 13. Monthly vegetation index and total precipitation	40
Figure 14. Regression analysis results.....	41
Figure 15. Crop yield during normal/moderate and ENSO years	43

List of tables

Table 1. Soil moisture station locations.....	14
Table 2. Climate mode description and phases	16
Table 3. Spatial location of gauged precipitation and temperature datasets.....	26
Table 4. Classification of ENSO	29
Table 5. Gauged and satellite soil moisture correlation	36

Acknowledgements

I express my deepest gratitude and appreciation to my supervisor Ronny Berndtsson and my co-supervisor Cintia B. Uvo for their constant support and guidance. I also want to thank Prof. Gerhard Barmen and Prof. Torleif Dahlin for the kindness and support mainly at the beginning of the program.

I would also like to extend my sincere gratitude to Teresa Soop and the Swedish International Development Cooperation Agency (SIDA). Thanks for having confidence and supporting young professionals from developing countries. Thanks to Ignacio Chirico and the staff at Departamento de Investigación Postgrado e Interacción Social (DIPGIS) at the Universidad Mayor de San Andres (UMSA) for the interaction with SIDA.

Thanks to the Institute of Hydraulics and Hydrology (IHH) of Bolivia, mainly Ramiro Pillco Zola, Angel Aliaga, and Nestor Funes. Also, special thanks to Francisco Rojas, Rubén Choque, and Pascual Mamani for their collaboration in fieldwork activities, and for being enthusiastic and positive, muchas gracias por todo compañeros.

Thanks to all the people at TVRL. The last years were a remarkable learning process, in which I met great professionals and friends. The time shared was substantial for my development. Tack så mycket!

I would like to thank Etzar Gómez, my colleague and partner in crime, thank you for your support, conversations, and innocent mischiefs.

Thanks to IIASA and the YSSP program 2017. In a period of disappointment in the academic system and science miscommunication with politicians, the YSSP program inspired me to remain positive and go forward with my research.

Thanks to Rolf and the TVRL book club, it was a great activity during the PhD. I enjoyed the interesting conversations and to know your life experiences.

I am lucky to be surrounded by people that supported and encouraged to culminate this program. Thanks to my husband Clement Naudin, Je t'aime. Thanks to my parents Julio and Teresa, siblings Beto, Jorge, and Danny, and the rest of my family. Gracias amada familia por ayudarme a cumplir mis sueños, por su cuidado y apoyo incondicional.

Popular summary

In 2016, Bolivia declared a state of emergency due to drought and water scarcity. While the city of La Paz had severe water shortages with partial inaccessibility to drinking water, the agricultural sector was the most affected. The Bolivian government reported almost 50% of crop production loss. And, Bolivia's second largest lake, Lake Poopó, dried up. Drought is a period drier than normal that is caused by a cumulative precipitation deficit during a certain period of time. A persistent drought, could affect streamflow, reservoir, and groundwater levels. In addition, precipitation deficit decreases the soil water content. Therefore, agriculture is often the first sector to be affected.

Drought is a disaster only when a system is unable to cope with its effects. To manage drought impacts, it is important to implement mitigation and preparedness measures. For this, a strong political commitment must be present, where stakeholders and decision makers are well informed and actively participate at the local and national level. This scenario is only possible after a clear comprehension of the problem. To understand the problem, analysis of the drought hazard and vulnerability is required. This can be used to define an early warning system, which can be used in drought preparedness.

To enhance the knowledge on water scarcity and drought, the objective of this study was to address the Bolivian Altiplano water scarcity for sustainable water management. For this, the changes of the rainfall that occurred in the past were analyzed. We assumed that the rainfall variance is related to global climate anomalies. For instance, the variability of temperature in the sea could affect the quantity of rain that falls. We found that higher temperature at the tropical Eastern Pacific Ocean decreases the occurrence of rain in the Altiplano. Less rain was also shown when the temperature in the North Atlantic Ocean was higher. This knowledge could help to forecast the rainfall.

The moisture in the soil is also very important for the water management. For instance, soil moisture analysis can help to understand the variability of agricultural production. Meaning that, if there is not enough water to cover the plant requirements, the crop production might decrease. And this decrease may affect economy and social conditions of the region, first of all farmers. Here, we studied the soil moisture in the Katari River Basin in the Bolivian Altiplano. We used a water balance model to estimate the soil moisture in two ways. The soil moisture was calculated based on the difference between water input and output. First, rainfall is the main water input and the output is represented by evaporation of the soil, transpiration of crops, runoff, and water moving out from the root zone. Second, the satellite moisture of the top soil layer, was used to estimate the soil moisture of the root zone, also based on evaporation of the soil, transpiration of crops, runoff, and

water moving out from the root zone. The results of both soil water balance models, firstly driven by precipitation and secondly driven by satellite soil moisture, were calibrated with gauged soil moisture. And finally, the soil moisture estimations were related to agricultural production, in order to seek the impact of soil moisture on crop yield.

After the precipitation and soil moisture analyzes, we studied the drought impact on agricultural production. For this, a vegetation index was used to estimate the quinoa and potato yield. Regions with adequate estimations were selected and compared to the rainfall and temperature. The findings indicate hotspots where the crop yield presents larger dependence of rainfall and temperature. The results of this study can assist to identify strategies for sustainable water management, motivate a proactive planning, and define mitigation policy measures.

In conclusion, the interactions among rain, temperature, and soil moisture were studied. We identified some of the causes and consequences of drier conditions in the Bolivian Altiplano. This information was related with agricultural production. And we could identify the hotspot regions where crop yield is more susceptible to droughts. The findings provide insights for sustainable water management.

Abbreviations

ADD	Accumulated Degree Days
AMM	Atlantic Meridional Mode
AMO	Atlantic Multidecadal Oscillation
CHIRPS	Climate Hazards Group InfraRed Precipitation
COI	Cone of Influence
CWT	Continuous Wavelet Transform
DP	Percolation
E	Nash-Sutcliffe Efficiency Coefficient
ENSO	El Niño-Southern Oscillation
ET	Evapotranspiration
ET _c	Crop Evapotranspiration
ET _o	Reference Evapotranspiration
FAO	Food and Agriculture Organization of the United Nations
FAR	False Alarm Ratio
FC	Field Capacity
GDD	Growing Degree Day
IRD	Institut de Recherche pour le Développement
ITCZ	Inter-Tropical Convergence Zone
K	Unsaturated Hydraulic Conductivity
K _c	Crop Coefficient
K _s	Water Stress Coefficient
K _{sat}	Saturated hydraulic conductivity
LST	Land Surface Temperature
MCA	Maximum Covariance Analysis
ME	Mean Error or Bias.
NAO	North Atlantic Oscillation
NDVI	Normalized Difference Vegetation Index
ONI	Oceanic Niño Index
P	Precipitation
p	Depletion Fraction
PCA	Principal Component Analysis
PDO	Pacific Decadal Oscillation
POD	Probability of Detection
R ²	Coefficient of Determination

RAW	Readily Available Soil Water Content
RH	Relative Humidity
RO	Surface Runoff
SCF	Squared Covariance Factor
SENAMHI	Servicio Nacional de Meteorología e Hidrología
SR	Solar Radiation
SST	Sea Surface Temperature
SW	Soil Moisture or Soil Water Content
TAW	Total Available Soil Water Content
T_b	Base Temperature
T_{dew}	Dew Point Temperature
TDPS	Titicaca Desaguadero Poopó and Coipasa Salt flat System
T_{mean}	Mean Temperature
TN	Minimum Temperature
TX	Maximum Temperature
UMSA	Universidad Mayor de San Andrés
WP	Wilting Point
WS	Wind Speed
WTC	Wavelet Coherence
XWT	Cross Wavelet Transform

Papers

Appended papers

- I. **Canedo-Rosso, C.**, Pillco Zolá, R., and Berndtsson, R., 2016. Role of hydrological studies for the development of the TDPS system. *Water* 8: 144. doi: 10.3390/w8040144.
- II. **Canedo-Rosso, C.**, Uvo, C.B., and Berndtsson R., 2019. Precipitation variability and its relation to climate anomalies in the Bolivian Altiplano. *Int. J. Climatol.* 39: 2096–2107. doi: 10.1002/joc.5937.
- III. **Canedo-Rosso, C.**, Nilsson, E., Duwig C., Gomez, E., and Berndtsson, R., 2019. Soil moisture estimation and crop yield response for the Katari River Basin in the Bolivian Altiplano (manuscript).
- IV. **Canedo-Rosso, C.**, Hochrainer-Stigler, S., Pflug, G., Condori, B., and Berndtsson, R., 2019. Drought risk in the Bolivian Altiplano associated with El Niño Southern Oscillation using satellite imagery data (manuscript under review in *J. Nat. Hazards Earth Syst. Sci.*).

Author's contribution to appended papers

- I. The author performed state of art review and wrote the major part of the manuscript. All the co-authors contributed in discussions and wrote minor parts of the manuscript.
- II. The author collected data and wrote the major part of the manuscript. The author and the co-authors developed the method, analysed the data, and discussed the results of the manuscript.
- III. The author collected data and wrote the major part of the manuscript. The author and the co-authors developed the method, analysed the data, and discussed the results of the manuscript.
- IV. The author collected data and wrote the major part of the manuscript. The co-authors wrote minor parts of the manuscript. The author and the co-authors developed the method, analysed the data, and discussed the results.

Other publications

Conference abstracts

- **Canedo-Rosso, C.**, and Berndtsson, R., 2018. Drought risk assessment on agriculture in the Bolivian Altiplano. Nordic Hydrological Conference 2018 - Nordic Water. Bergen, Norway.
- **Canedo-Rosso, C.**, Uvo C.B., and Berndtsson, R., 2016. Precipitation variability over the eastern Bolivian Altiplano. EGU General Assembly. Vienna, Austria.
- **Canedo-Rosso, C.**, Uvo C.B., and Berndtsson, R., 2015. Variabilidad espacial de la precipitación en el Altiplano Boliviano. Conferencia Nacional de Especialistas en Sistemas de Información Geográfica y Teledetección aplicado a cuencas y recursos hídricos. Ministerio de Medio Ambiente y Agua. La Paz, Bolivia.
- **Canedo-Rosso, C.**, and Berndtsson, R., 2015. Flash floods in the Andean highlands: International SWAT Conference. Pula, Sardinia, Italy.

Reports

- **Canedo-Rosso, C.**, 2017. Drought impacts and risks on agricultural production in the Bolivian Altiplano. Young Scientists Summer Program (YSSP). International Institute for Applied Systems Analysis (IIASA). Laxenburg, Austria.

Abstract

Water scarcity is a consequence of complex interactions between water access and water use. In fact, the time period over which precipitation deficit accumulates is a determining factor for the occurrence of drought. Drought induces crop production losses and far-reaching societal effects. In the South American Altiplano, drought is a major hazard. Here, drought leads to food shortages, malnutrition, migration, loss of biodiversity, and local conflicts. In order to improve the drought resilience and develop mitigation and adaptation strategies, there is a need to study water scarcity episodes, and their drivers in the Bolivian Altiplano. Therefore, the main goal of this study was to address water scarcity in the Bolivian Altiplano for sustainable water management. In the first instance, previous research on the subject was synthesized in a state of art with respect to climate and water resources. Secondly, analysis of precipitation variability, and its relation with climate phenomena were performed. It involved the analysis of the long-term austral summer precipitation variance at six locations in the Bolivian Altiplano. The precipitation variability was related to climate anomalies over the Pacific and Atlantic Oceans. The results show significant negative relationship between summer precipitation and climate phenomena in the studied region. Thirdly, a hydrological study to define the soil moisture characteristics was initiated in a river basin of the Bolivian Altiplano. It involved soil moisture estimations using soil water balance and derived satellite approaches. The estimated soil moisture was compared and validated with gauged soil moisture. The soil moisture estimations were used to define the impact of water scarcity in the agricultural production. Finally, a drought risk analysis based on the association of precipitation and temperature variability with quinoa and potato yield was accomplished. For this, monthly satellite data of precipitation and temperature were validated with gauged data. The precipitation and temperature were related with agricultural data in the studied region. The normalized difference vegetation index was used to estimate the crop yield of the agricultural area. It was found that the variance of the agricultural production depends largely on the precipitation and temperature variance. The findings of this thesis provide insights in identifying strategies to improve the water management in the Bolivian Altiplano, mainly during water stress conditions. Moreover, the analyses enhance the knowledge for seasonal forecasting, drought disaster risk management, proactive planning, and mitigation policy measures in vulnerable regions of the Bolivian Altiplano.

Resumen

La escasez de agua es consecuencia de complejas interacciones entre acceso y uso del agua. De hecho, el período de tiempo en el que el déficit de precipitación es acumulado es un factor determinante para la ocurrencia de un evento de sequía. La sequía provoca pérdidas en la producción de cultivos, con efectos sociales de gran alcance. En el Altiplano de Sud América, la sequía un fenómeno climático de gran importancia. La sequía induce la escasez de alimentos, desnutrición, hambruna, migración, pérdida de biodiversidad y conflictos a nivel local. Para mejorar la resiliencia a la sequía y desarrollar estrategias de mitigación y adaptación, es necesario estudiar los eventos de escasez de agua y sus causas. Por lo expuesto, el objetivo de este estudio fue abordar la escasez de agua del Altiplano de Bolivia, para lograr un manejo sostenible de los recursos hídricos. En primera instancia, se realizó una síntesis de previas investigaciones con respecto al clima y recursos hídricos. Posteriormente, se realizó un análisis de variabilidad de la precipitación en relación con los fenómenos climáticos. En este estudio se evaluó la variación de la precipitación durante el verano austral en seis lugares del Altiplano boliviano. Esta variabilidad fue relacionada con seis anomalías climáticas. Los resultados muestran una significativa relación negativa entre la precipitación y los fenómenos climáticos. Posteriormente, un estudio hidrológico fue realizado para definir las características de humedad del suelo en una cuenca del Altiplano. Las estimaciones de humedad del suelo incluyeron el balance de hídrico y el derivado de datos satelitales. Las estimaciones de humedad del suelo fueron comparadas y validadas con datos de humedad medidos en campo. Finalmente, se relacionó el rendimiento de la quinua y la papa con la precipitación y temperatura. Para este estudio, los datos de precipitación y temperatura medidos en campo se validaron con los datos satelitales. Los datos de precipitación y temperatura se relacionaron con datos agrícolas en la región estudiada. El índice de vegetación se utilizó para estimar el rendimiento de los cultivos en el área agrícola. Como resultado de esta investigación, se encontró que la variación de la producción agrícola depende en gran medida de la variación de precipitación y temperatura. Los resultados de esta tesis proporcionan información para identificar estrategias para mejorar la gestión del agua en el Altiplano boliviano, principalmente durante las condiciones de estrés hídrico. Además, los análisis aportan al conocimiento de predicciones de datos climáticos, la gestión del riesgo de desastres por sequía, la planificación proactiva y las medidas de mitigación en las regiones vulnerables del Altiplano boliviano.

1. Introduction

The Altiplano is situated in the central part of the Andes mountain chain in South America, in which diverse native cultures have inhabited during thousands of years. Here, human activities have continuously been affected by climate variability and water availability (Buytaert and De Bièvre, 2012). The summer rainfall represents more than 70% of the total annual precipitation (Canedo-Rosso et al., 2019b; Garreaud et al., 2003). And, it is associated with the South American Monsoon (Zhou and Lau, 1998) that shows a prevalence for easterly winds. The rainy season represents the major source of water for drinking purposes, agriculture, streamflow, and groundwater recharge (Morales et al., 2012). Agricultural production is directly affected by climate hazards in the Altiplano, for instance, drought conditions lead to shortage of food for humans and animals (Garcia, 2003; Garcia et al., 2007). This is the case for the most important crops in the Altiplano: quinoa and potato, which are affected by precipitation variability and losses in crop production due to drought (Garcia et al., 2003). The socio-economic impacts of drought are broad and the consequences can cause malnutrition, starvation, migration, biodiversity loss, and local conflicts (UNISDR, 2009). More specifically, droughts in the Altiplano cause losses in crop and livestock, and force inhabitants' migration (World-Bank, 2009). For example, a drought caused by the El Niño 1997–1998 caused a loss of USD 530 million in Bolivia, 53% of which stemmed from drought (CAF, 2000). More recently, in 2015–2016 drought affected 665,000 people and over USD 450 million of losses were reported (Guha-Sapir et al., 2016). As a consequence, the water supply was temporarily interrupted because of the low water level in reservoirs in the major cities of Bolivia: La Paz and El Alto (Marengo et al., 2017). Moreover, the Lake Poopó, the second largest lake in the region, dried up affecting the local biodiversity and economic activities (Satgé et al., 2017).

In order to improve the drought resilience and develop mitigation and adaptation strategies, there is a need to study water scarcity episodes, and their drivers in the Bolivian Altiplano. Therefore, the main goal of this study was to address the Bolivian Altiplano water scarcity for sustainable water management. For this purpose, we analysed precipitation variability, and its relation with climate phenomena. Then, we performed a hydrological study to define the soil moisture content. Finally, we studied the drought risk based on associations with precipitation and temperature variability and effects on quinoa and potato yield. The findings of

this study provide insights to identify strategies to improve the water management in the Bolivian Altiplano, mainly during water stress conditions. Moreover, the results enhance the knowledge on hydro-climatological variability in the Altiplano for drought disaster risk management, proactive planning, and mitigation policy measures in vulnerable regions.

The specific objectives of this study were:

- to produce a state of the art review of research with respect to climate and water resources in the TDPS hydrological system, define important research gaps in hydrological data information of the region, and the key role that these have for the sustainable development in view of climate change and population increase (**Paper I**),
- to analyse the precipitation variability and its relation with climate anomalies such as the ENSO, PDO, NAO, AMM, and AMO on the austral summer precipitation over the Bolivian Altiplano (**Paper II**),
- to estimate the soil moisture and crop yield response of the Katari River Basin in the Bolivian Altiplano (**Paper III**),
- to address the corresponding question how a risk-based approach can determine the potential need of resources during drought and provide possible solutions how to determine hotspot areas where it is most likely that such resources would be needed (**Paper IV**).

2. Theoretical background

Water availability plays a fundamental role in many natural and societal processes. Water scarcity occurs where there are insufficient water resources to satisfy the water demand. It can refer to long-term imbalance, as a result of exceeding level of water demand against the water availability affecting the water supply capacity. In arid and semiarid areas, the impact of drought can be exacerbated due to low water resources availability. For this, there is a need to improve the knowledge of water scarcity and drought processes to strengthen the resilience and develop mitigation and adaptation strategies. This chapter gives a theoretical background of the physical processes of water scarcity and drought in the Bolivian Altiplano.

2.1. Climate variability

The rainy season in the Altiplano occurs generally from December to March, and the dry season from May to August (UNEP, 1996). The austral summer precipitation represents over 70% of the total annual precipitation (Canedo-Rosso et al., 2019b; Garreaud et al., 2003). The Altiplano summertime (DJFM) precipitation variability was investigated by among others Thibeault et al. (2012), Lenters and Cook (1999), Vuille et al. (2000), and Garreaud and Aceituno (2001). Easterly winds transport humid air from the lowlands east of the Altiplano to the region, while the prevalence of westerly winds inhibits moisture transport (Lenters and Cook, 1999; Thibeault et al., 2012; Vuille et al., 2000). In more detail, during the austral summer months (DJF) the low-level flow, transports warm and wet air from the Amazon Basin to the subtropics (Garreaud, 2000). During these months, the Bolivian High is established over the Altiplano (Lenters and Cook, 1997). The Bolivian High is an upper-level anticyclone over the central Andes. The southward displacement of the Bolivian High is associated with low-level north-westerly air flow and humid, unstable conditions that are favourable for convection in the Altiplano (Thibeault et al., 2012). During the austral summer, establishment of the upper-level Bolivian High is centred at 17°S and 70°W (Garreaud, 2009). Contrary, during winter months (JJA) and dry spells (e.g., El Niño events) westerly flow prevails, and the Bolivian High is weak (Vuille, 1999). Thus, the occurring precipitation is low. Precipitation in the Altiplano presents a northeast-southwest gradient. This means a decreasing

annual precipitation from above 800 mm in the north-eastern to below 200 mm in the south-western Altiplano (Vuille et al., 2000). The largest rainfall occurs around the Lake Titicaca (CMLT, 2014), with an annual precipitation from 800 to 1400 mm (UNEP, 1996). The annual precipitation in the northern Lake Poopó is about 420 mm, and 270 mm in the south (Pillco and Bengtsson, 2006). The precipitation dramatically decreases in the Atacama Desert, where the annual rainfall is almost zero.

The El Niño-Southern Oscillation (ENSO) is the most reported climate mode associated with the Altiplano climate variability (see Aceituno, 1988; Ronchail and Gallaire, 2006; Thompson et al., 1984; Vuille, 1999). The ENSO is a periodical variation in sea surface temperature (SST) due to the interaction between the atmosphere and ocean over the tropical eastern Pacific Ocean. This results in dryer or wetter conditions over the course of a 2–7 year period. The ENSO presents three phases: neutral, warm (El Niño), and cold (La Niña). In the Altiplano, the El Niño is generally related to dryer and warmer conditions, and the La Niña regularly represents the opposite effects, which are cooler and wetter conditions (Garreaud et al., 2003; Garreaud and Aceituno, 2001; Thibeault et al., 2012).

The Pacific Decadal Oscillation (PDO) is another important phenomenon affecting climate variability. PDO oscillates with a longer frequency than the El Niño-like pattern (Zhang et al., 1997), with a multidecadal fluctuation in the Pacific Ocean (Mills and Walsh, 2013). PDO is the leading principal component of the North Pacific SST variability. Precipitation variability in South America tends to be stronger when ENSO and PDO phases coincide, and weaker when their phases differ (Kayano and Andreoli, 2007). PDO presents a decadal and inter-decadal variability of precipitation in South America, which is similar to ENSO in spatial structure, but its amplitude is lower (Garreaud et al., 2009).

Climate variability in the Altiplano is not only associated with anomalies originating in the Pacific Ocean, but also in the Atlantic Ocean. The NAO is an oscillation of atmospheric pressure at sea level between the Icelandic low and the Azores high (Walker and Bliss, 1932). The NAO shows seasonal and inter-annual variabilities with positive and negative phases (Mächel et al., 1998). Both phases are associated with the variability of precipitation, temperature, and storms over the Atlantic Ocean and surrounding continents (Marshall et al., 2001).

The AMM and the AMO are associated with the ocean-atmosphere variability in the tropical and North Atlantic, respectively (Chiang and Vimont, 2004; Kerr, 2000; Schlesinger and Ramankutty, 1994; Xie and Carton, 2004). The AMM shows an inter-annual variability (Knight et al., 2005). And the AMO varies on multi-decadal timescales, with an oscillation of about 70 years (Schlesinger and Ramankutty, 1994). The AMM and AMO are characterized by variation of the SST and a shift of the intertropical convergence zone (ITCZ) position (Grossmann and Klotzbach,

2009; Vimont and Kossin, 2007). The ITCZ shift is caused by warmer SST and weak easterly wind flow in the northern tropical Atlantic, and cooler SST and stronger easterly wind flow in the southern tropical Atlantic (Chiang and Vimont, 2004; Smirnov and Vimont, 2011). During summer months (DJFM), the ITCZ position and the formation of the Bolivian High result in a prevalence of easterly winds over the Altiplano (Garreaud et al., 2003). This condition defines the rainy season in the South American Altiplano.

2.2. Water content in the soil

The water content in the soil involves various parameters of the water budget, including outflow, inflow, and changes in storage (Fig 1). The water inflows are rainfall, irrigation, surface water inflow, and capillary rise of groundwater. While, the outflows are soil evaporation, crop transpiration, surface outflow, and percolation. The soil can be defined as the water reservoir for plants (Allen et al., 1998). The soil water availability depends on the capacity of the soil to retain moisture. Field capacity, is the amount of water that the soil hold against gravitational forces with a tension of about 33 kPa. The water content above field capacity is not held by the soil. If water is not supplied, the content of water in the soil decreases as a result of evapotranspiration. When the soil reaches the wilting point, the force of the water retained in the soil inhibits the plant accessibility to water. The water held to soil particles has a tension of about 1500 kPa when it reaches the wilting point. And the plant will permanently wilt. The amount of water between field capacity and wilting point is considered as the total water available (TAW) for the plant.

The evapotranspiration is the combination of the soil surface evaporation and the crop transpiration. The solar radiation, air temperature, relative humidity, and wind speed are the main factors that affect the evapotranspiration. The reference crop evapotranspiration (ET_o) represents the evapotranspiration from a hypothetical grass crop. The ET_o determines the evaporative demand of the atmosphere independently of crop type and soil factors. The FAO Penman-Monteith method (Eq. (4)) incorporates the aerodynamic and the surface resistance factors (Allen et al., 1998). Penman (1948) developed the combination method by combining the energy balance with the mass transfer methods from an open water surface. The surface resistance describes the resistance of vapour flow through the crop and soil surface. The aerodynamic resistance describes the resistance from the vegetation surface and air friction. The Penman-Monteith approach includes parameters that govern the energy exchange between a specific type of vegetation and atmosphere. The FAO Penman-Monteith method defines a hypothetical crop of 0.12 m height with a surface resistance of 70 s m^{-1} , and an albedo of 0.23.

The crop evapotranspiration (ET_c) refers to the evaporating demand from crops. The effects of the crop characteristics to the evapotranspiration are integrated into the crop coefficient (K_c). These characteristics are crop height, surface albedo, canopy resistance, and exposed soil evaporation. K_c varies over the phenological stage of the crop. The K_c reaches its maximum at mid-stage, when the plant cover is developed. The K_c of quinoa under no water stress is 0.52 at initial stage, 1.0 at mid-stage, and 0.7 at late stage (Garcia et al., 2003). The initial stage starts from planting to 10% of ground cover, the crop development starts from 10% of ground cover to full cover, mid-stage starts from full cover to maturity start, and late stage starts from maturity to harvest or full senescence (Allen et al., 1998).

The crop water requirement is defined as the amount of water that the plant needs to be supplied to compensate the evapotranspiration loss (Allen et al., 1998). The ET_c under water stress conditions represents the difference between the crop water requirement and effective precipitation. In theory, water is available for the plant from field capacity until wilting point, but the crop water uptake is reduced before reaching the wilting point. This occurs when the soil matrix force to retain water is higher than the plant capacity to extract water. The water that can be extracted by the plant is the readily available water (RAW), which is a fraction of the total available water (TAW). The depletion fraction, p , varies over the crop and evaporation power of the atmosphere. For quinoa, p is about 0.61 (Garcia, 2003). The effects of soil water stress on crop can be represented by the water stress coefficient, K_s . At field capacity the K_s is equal to 1. When the content of water in the soil is lower than RAW, K_s decreases. At wilting point the K_s is equal to 0.

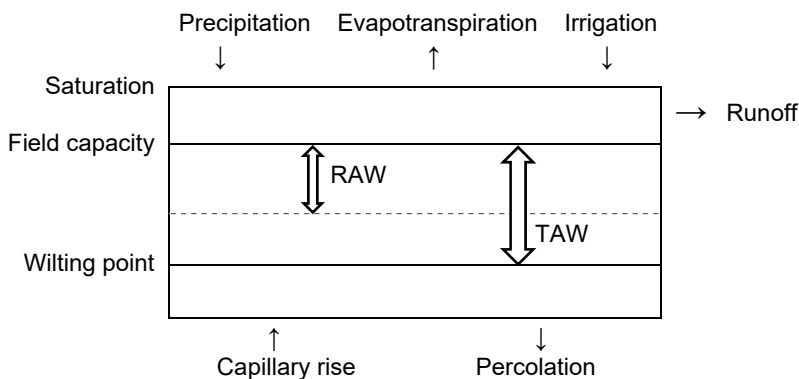


Figure 1. The soil water balance
Adapted from Allen et al. (1998).

Percolation refers to water in the soil profile moving out from the rooting zone, and it occurs when the water content in the soil exceeds field capacity. The travel time for percolation is the water in excess of the field capacity in relation to the unsaturated hydraulic conductivity (Savabi and Williams, 1995). And, the hydraulic conductivity is the capacity of the soil to conduct water, and it can be calculated based on soil physical properties such as soil texture and organic matter (Saxton and Rawls, 2006).

2.3. Drought

Droughts originate from a deficiency of precipitation, and can result in water shortages. However, water availability depends not only on natural factors, but also on human activities (Wilhite and Glantz, 1985). Sometimes, precipitation deficiency coincides with periods of high temperature, low humidity, and high wind speed. This scenario could induce a reduction of soil moisture, and water level of rivers and lakes. However, the drought itself is not a disaster (WMO, 2006) since it depends on the impact on people, economy, and environment. Moreover, a region could be resilient to droughts and thus, reduce negative impacts.

2.3.1. Drought concept and types

The specific hydrological processes, socioeconomic structure, and water demand of a particular region make it challenging to uniquely define drought (Mishra and Singh, 2010). Moreover, drought is a complex phenomenon that may involve lower than normal rainfall affecting economic, social, and environmental sectors at different time scales (Hagman et al., 1984). The World Meteorological Organization (WMO) defines drought as a natural hazard caused by extended deficiency of precipitation, which is insufficient to meet the demand of human activities and environment (WMO, 2006). Prolonged precipitation deficit could reduce stream flow, reservoir levels, and groundwater recharge. In consequence, soil moisture could decrease and affect agricultural production. Commonly, four types of drought can be described (Fig. 2): meteorological, hydrological, agricultural, and socioeconomic drought (Mishra and Singh, 2010; Wilhite and Glantz, 1985; WMO, 2006). Meteorological drought is usually defined as precipitation deficiency during a certain time period. Agricultural drought occurs when soil moisture is insufficient to meet crop water requirements. Hydrological drought occurs when water deficiency affects surface and groundwater. Finally, socio-economic drought affects human activities by a reduced precipitation and water availability.

Meteorological drought is commonly calculated based on precipitation anomalies. The WMO indicates normal precipitation as the average of precipitation in a period of 30 years. Some researchers define meteorological drought as a lower precipitation than normal (e.g., Shukla et al., 2015). Other approaches analyse the drought using the duration, intensity, and frequency of accumulated precipitation in relation to water shortages (e.g., Spinoni et al., 2014). Other researchers evaluate a meteorological drought based on indicators and indices (see Heim, 2002; Yihdego et al., 2019). For instance, the identification of dry spells can be done using a standardized precipitation index (McKee et al., 1993). Since, drought greatly depends on atmospheric circulation and local conditions, its definition and calculation vary depending on region.

If the deficit of precipitation is prolonged, an agricultural drought might occur. Here, the availability of water in the soil is insufficient to support crop development (Huang et al., 2014b). However, agricultural drought varies depending on many factors. For instance, the capacity of the soil to hold water and the infiltration rates vary, depending on initial soil moisture condition, slope, and soil type (WMO, 2006). In addition, crops present different level of tolerance to drought depending on biological characteristics, stage of growth, and physical and biological properties of the soil (Botterill and Fisher, 2003).

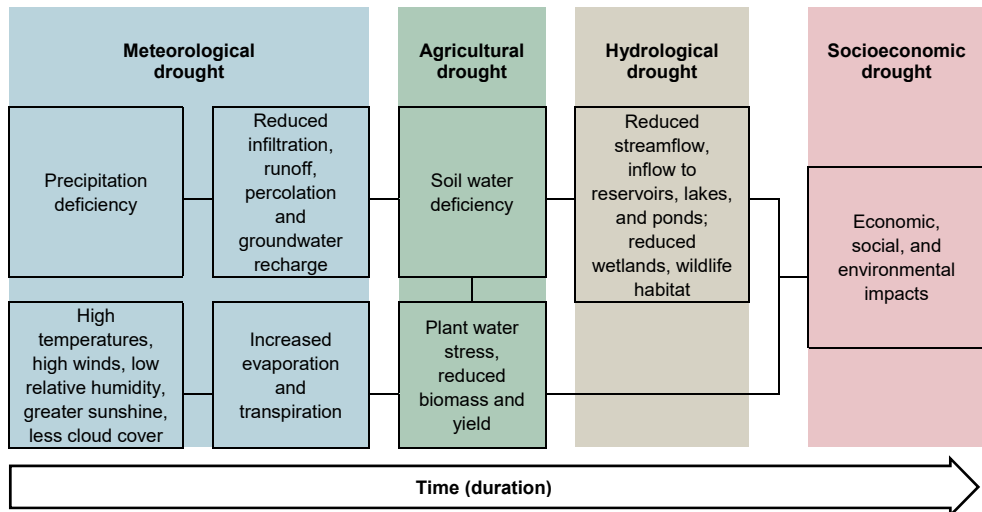


Figure 2. Drought occurrence and impacts
 Source: National Drought Mitigation Center, University of Nebraska-Lincoln, USA.

Hydrological drought can affect water bodies that are used for multiple purposes, such as irrigation, recreation, navigation, hydropower, and drinking water (Smakhtin, 2001). An insufficient availability of water for actual demand could escalate social conflicts between water users. This situation may lead to a socioeconomic drought. Socioeconomic drought may occur when the demand for an economic good exceeds supply as a result of a weather-related shortfall in water supply (Sandford, 1979). This type of drought depends on time and space processes of supply and demand.

2.3.2. Global and local context of drought

Agricultural production is highly sensitive to climate hazards, including droughts and heat waves. Losses due to drought events represent a significant challenge to farmers, stakeholders, and governments worldwide (UNISDR, 2015). Worryingly, the scientific community predicts an amplification of these negative impacts due to future climate change (IPCC, 2013). Drought impact varies depending on timescale, hazard intensity, and capacity to prevent and respond to this hazard (UNISDR, 2009). Regarding prevention aspects, diverse strategies and policies aim to reduce the socioeconomic and environmental consequences of drought events (WMO, 2006), including the setup of insurance and irrigation systems. Governments have to take a leading role in the implementation of strategies for future drought risk (Lal et al., 2012). Indeed, the recent Sendai Framework for Disaster Risk Reduction (SFDRR) agreement was developed to significantly reduce global disaster mortality, number of affected people, economic loss, and damage to critical infrastructure and disruption of basic services due to natural disasters (including droughts) by 2030. The agreement explicitly recognizes the need for governments to take a primary role in reducing disaster risk with support of relevant stakeholders (UN, 2015). The SFDRR explicitly calls for an increase in the availability and access to disaster early warning systems. In fact, drought early warning systems are essential components for drought preparedness and resilience because they can provide information to water-sensitive sectors such as farming in a timely manner.

The Sustainable Development Goals (SDGs) state that the priority areas for adaptation to climate change are water and agriculture. These in turn, are related to the largest climate hazards that are floods, drought, and higher temperature (UN, 2016). Additionally, implementation of early warning is fundamental for drought disaster risk management, proactive planning, and mitigation policy measures in vulnerable regions, including Latin American countries such as Bolivia (Verbist et al., 2016). As in most cases in developing countries, data scarcity is a major issue for monitoring, tracking progress, and the evaluation of risk reduction strategies (major goals within the SFDRR and SDGs; see UN, 2015, 2016).

Regarding droughts in Bolivia, climate variability in the Altiplano is strongly associated with the El Niño Southern Oscillation (ENSO), and droughts are generally driven by the ENSO warm phases (Garreaud and Aceituno, 2001; Thompson et al., 1984; Vicente-Serrano et al., 2015). Generally, agricultural productivity in the Altiplano is low due to high susceptibility to climate and poor soil conditions (Garcia et al., 2007). Poor agricultural production is associated with the ENSO climate phenomena (Buxton et al., 2013). Apart from that, high evaporative demand and erratic distribution of rainfall increase agricultural vulnerability significantly. In addition, precipitation dependency for rainfed agriculture and frost risk limit farming production to the austral summer (Condori et al., 2014; Garcia et al., 2007). Large socio-economic losses have been experienced in the past in Bolivia due to ENSO. For example, 135,000 people were affected and USD 515 million loss were registered in 1997–1998 (UNDP, 2011). More recently, 665,000 people were affected and over USD 450 million of losses in 2015–2016 were experienced (Guha-Sapir et al., 2016). To lessen the long-term impacts of these events, the national government has allocated large budget amounts for emergency operations to compensate part of the losses, which are usually evaluated in an ex-post fashion. Important in our context is that Bolivia has implemented a national program for risk disaster management that includes an early warning system that informs about disaster occurrence a few days ahead of the event.

3. Study area

The Altiplano (15–22°S) is located in the central part of the Andes mountain chain in South America. Based on the last national census in Bolivia in 2012, the Bolivian Altiplano has about 2,000,000 inhabitants (INE, 2015b). The Altiplano extends from western Bolivia, southern Peru, and northern Chile and Argentina (Fig. 3). This endorheic basin contains two large lakes, Lake Titicaca and Lake Poopó. The two lakes are connected through the Desaguadero River, which is the only outlet of Lake Titicaca. The Lake Titicaca is the largest freshwater lake in the continent with a surface area of 8,400 km², a volume of 932 km³ (Revollo, 2001), and a maximum depth of 281 m (Richerson et al., 1977). It represents one of the main permanent sources of water for agriculture, forestry, fishing, and other activities in the region (UNESCO-WWAP, 2003). The Lake Poopó has an average surface area of 3,000 km² and a maximum depth of 3 m (Pillco and Bengtsson, 2006). The Lake Poopó has dried out several times in the past. In 2016, it dried out due to water use and lower precipitation than normal (Satgé et al., 2017). This caused significant socio-economic and environmental losses, directly affecting fishers, endemic species, and exposing mining sediments deposited in the lake. On the other hand, the overflow from Lake Poopó during wet years ends up in the Coipasa Salt Pan (Revollo, 2001), which in turn drains to Uyuni Salt flat through the Laca Jahuirra River. The Uyuni Salt flat is the world's largest salt flat that was formerly occupied by lakes. High insolation in the region causes large evaporation losses from these lakes, and in consequence a deposition of lacustrine sediments, that determined the formation of the salt flat (Baker et al., 2001). Finally, the Atacama Desert is located in the southwestern Altiplano, which is the driest desert in the world. In consequence, the northern Altiplano shows a wetter environment than the arid southern part.

Within the Bolivian Altiplano, the Katari River sub-basin is located in southern Lake Titicaca Basin. It has an area of 654 km². It covers 11% of the total population of Bolivia (BID, 2016). The annual precipitation is about 480 mm in the southwestern part of the sub-basin and 620 mm in the north-eastern part (MMAyA, 2010). Here, the main economic activity is agriculture, and the water demand is mainly for drinking water and irrigation. However, evapotranspiration is the major water loss component.

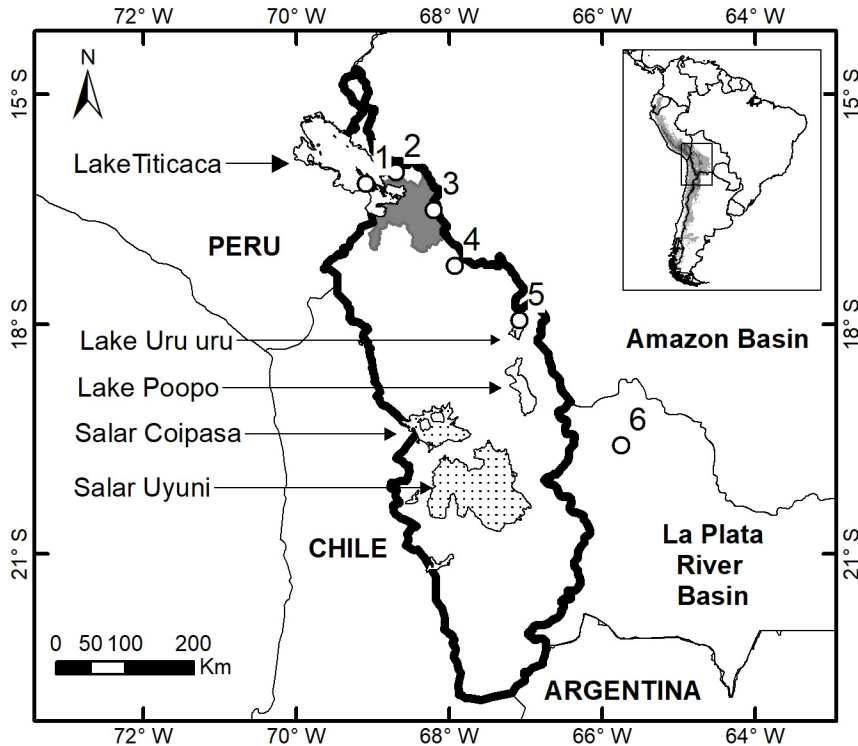


Figure 3. The Bolivian Altiplano in South America

The Bolivian Altiplano located in the central part of the Andes mountain chain in South America is represented by a thick solid black line (**Papers I and IV**). The gauged precipitation at six locations is represented with white circles: (1) Copacabana, (2) El Belen, (3) El Alto, (4) Patacamaya, (5) Oruro, and (6) Potosi Los Pinos (**Paper II**). The Katari River sub-basin is shown as a shaded area (**Paper III**).

In the Altiplano, important indigenous civilizations have emerged including the Inca and Tiwanaku. These civilizations domesticated plants and animals such as potato, quinoa, and lama (Erickson, 1988; Repo-Carrasco-Valencia and Serna, 2011). Nowadays, agriculture is still one of the main economic activities. However, crop production is limited to the summer due water constraints and climate conditions, e.g., frost (García et al., 2007). Less than 9% of the agricultural area are irrigated in Bolivia (INE, 2015a). Therefore, precipitation is the main source of water for agricultural production. Common agricultural production in the area is focused on crops, fishing, and cattle (UNESCO-WWAP, 2003). Quinoa and potato are two of the most important crops in the Altiplano. Due to the fact that farming is mostly rainfed, climate related phenomena are very important for crop production.

4. Data

4.1. Precipitation and temperature

Time series of daily and monthly precipitation and maximum, and minimum temperature were supplied by the Servicio Nacional de Meteorología e Hidrología (SENAMHI) de Bolivia.

- Analysis of precipitation variability (**Paper II**) included the summer precipitation (DJFM) totals from 1948 to 2016 at six locations in the Bolivian Altiplano: Copacabana, El Belen, El Alto, Patacamaya, Oruro, and Potosi Los Pinos (Fig. 3).
- Analysis of the soil moisture variability was performed for the Katari River sub-basin (**Paper III**). The Katari River sub-basin is located in the south-eastern Lake Titicaca Basin (Fig. 4). Available data included daily precipitation and maximum, and minimum temperature from 1981 to 2017 from the Servicio Nacional de Meteorología e Hidrología (SENAMHI) of Bolivia. Daily precipitation was used from El Alto (16° 30' 37"S, 68° 11' 55"W), Tambillo (16° 34' 0"S, 68° 30' 0"W), and Viacha (16° 39' 30"S, 68° 16' 55"W). Daily maximum and minimum temperature were used from El Alto, and Viacha. Daily precipitation from the Institut de Recherche pour le Développement (IRD) from 2013 to 2017 was also available at 6 studied sites described in Table 1, and maximum and minimum temperature for Alto Lima and Tambillo from the same time period.
- Drought risk analysis for quinoa and potato was analysed in the agricultural land area of the Bolivian Altiplano (**Paper IV**). Satellite based monthly rainfall and temperature datasets from September 1981 to August 2015 were used in the analysis. The details of the satellite data are explained below. The validation of the satellite data was developed using gauged datasets of monthly precipitation at 23 locations as well as maximum, and minimum temperature at 11 locations in the Bolivian Altiplano.

It should be noted that the precipitation gauges have an uneven spatial distribution and are mainly concentrated to the northern Bolivian Altiplano. To improve the spatial coverage of rainfall data, monthly quasi-rainfall time series from satellite data were included in our study. The Climate Hazards Group InfraRed Precipitation

with station data (CHIRPS) quasi-global rainfall dataset was used. CHIRPS presents a 0.05° resolution satellite imagery and is a quasi-global rainfall dataset from 1981 to the near present with a satellite resolution of 0.05° (Funk et al., 2015). CHIRPS dataset builds on interpolation techniques and high resolution, long period of record precipitation estimates based on infrared Cold Cloud Duration (CCD) observations. CCD values are a measure of the amount of time a given pixel has been covered by high cold clouds. CHIRPS uses the Tropical Rainfall Measuring Mission Multi-Satellite Precipitation Analysis (TMPA 3B42) 2000–2013 with 0.25° of resolution to calibrate global Cold Cloud Duration (CCD) rainfall estimates.

Monthly mean land surface temperature (LST) was obtained from the Global Historical Climatology Network and the Climate Anomaly Monitoring System from the US National Oceanic and Atmospheric Administration (NOAA, <https://www.esrl.noaa.gov/psd/data/gridded/data.ghcncams.html>). The LST has a resolution of 0.5° and it is conveniently also available during the study period from September 1981 to August 2015. CHIRPS is described in detail at <http://chg.geog.ucsb.edu/data/chirps/>.

4.2. Other hydrological variables

Daily gauged soil moisture data were obtained from the IRD during 2013 to 2017 at 6 sites (Table 1, Fig. 4). Here, the soil moisture sensors measure the volumetric water content in the soil (m^3m^{-3}) at 250 and 750 mm of soil depth for San Gabriel, 300 and 800 mm for Alto Lima, 250 and 700 mm for Brabol, 200 and 700 mm for Puchukollo, 200 and 700 mm for Viacha-IBTEN, and 50 and 200 for Tambillo. And daily satellite-based soil moisture data were obtained from the ESA CCI SM v04.4 that comprises the active (scatter-meter), passive (radiometer), and combined satellite soil moisture datasets with a time span from 1981 to 2017 with a satellite resolution of 0.25° and a soil layer depth of 0.5–2 cm. The soil hydraulic properties were quantified based on the soil texture (content of sand, silt, and clay) and organic matter at each soil layer, based on the soil profile data obtained from the IRD.

Table 1. Soil moisture station locations

	Station	Latitude (°S)	Longitude (°W)	Altitude (m)
1	San Gabriel	16°25'19.51"	68°10'27.30"	4310
2	Alto Lima (EPSAS)	16°27'19.88"	68°09'42.81"	4265
3	Brabol	16°29'15.52"	68°13'16.81"	4050
4	Puchukollo	16°32'00.64"	68°15'05.52"	3950
5	Viacha (IBTEN)	16°39'26.12"	68°16'54.68"	3870
6	Tambillo	16°31'15.31"	68°30'18.30"	3840

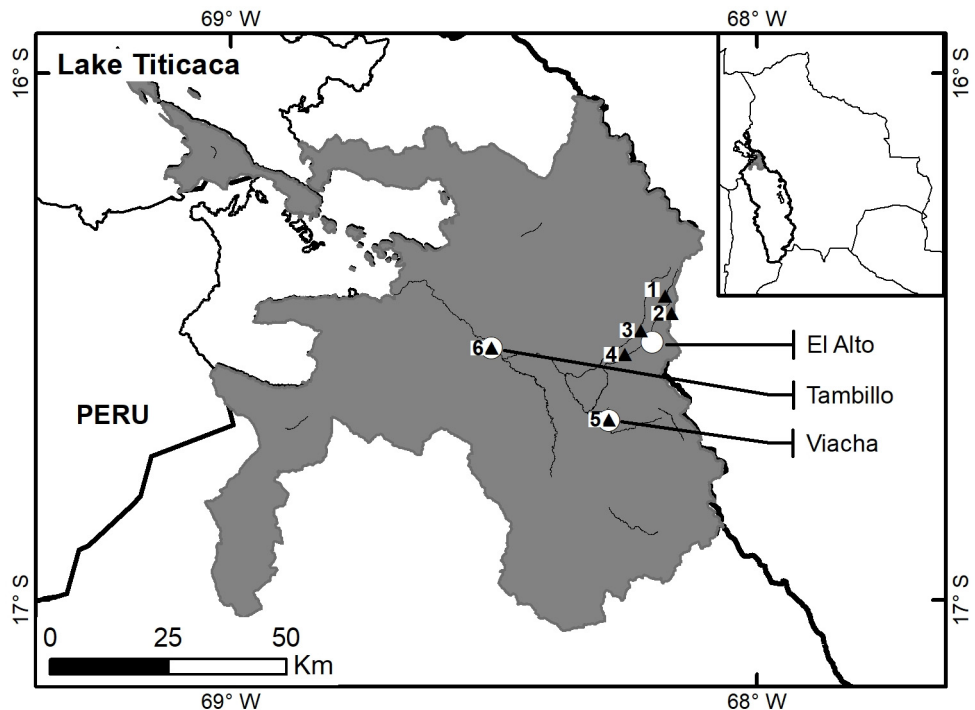


Figure 4. Katari River sub-basin in the Bolivian Altiplano

The Katari River sub-basin located in the southern Lake Titicaca (shaded area). The studied locations are (1) San Gabriel, (2) Alto Lima (EPSAS), (3) Brabol, (4) Puchukollo, (5) Viacha (IBTEN), and (6) Tambillo. The soil moisture and precipitation gauges are denoted by triangles. The weather stations are El Alto, Tambillo and Viacha (white circles).

Time series of wind velocity, and relative humidity were obtained for El Alto (1981–2017) and Viacha (1981–2015) from the SENAMHI. Wind velocity, relative humidity, and solar radiation data were obtained for Alto Lima and Tambillo from 2013 to 2017 from the IRD. The time series were synchronized at the closest spatial location to obtain a continuous daily dataset from September 1981 to August 2017 for the 6 studied locations (Table 1).

4.3. Climate modes of variability

Monthly indices of Niño3.4 and Niño3, PDO, NAO, AMM SST, and AMO were obtained from the US National Oceanic and Atmospheric site (NOAA, <https://www.esrl.noaa.gov/psd>). Monthly means were averaged seasonally for DJFM from 1948 to 2016. The climate modes of variability that included in the study are described in Table 2.

Table 2. Climate mode description and phases

Based on Canedo-Rosso et al. (2019b). * denotes very strong El Niño events.

Mode	Definition and periodicity	Negative phase	Positive phase
Niño3.4 and Niño3: El Niño Southern Oscillation (see Null, 2018)	Inter-annual variability of tropical Pacific SST. Periodicity of 2–7 years	Strong La Niña events: 1955–1956, 1973–1976, 1988–1989, 1998–2000, 2007–2008, 2010–2012	Strong and * very strong El Niño events: 1957–1958, 1965–1966, 1972–1973, 1982–1983*, 1986–1988, 1990–1995, 1997–1998*, 2015–2016*
PDO: Pacific Decadal Oscillation (see Mantua and Hare, 2002; Mantua et al., 1997; Minobe, 1999)	Multi-decadal variation in the Pacific SST. Periodicity of 15 to 25 years and 50 to 70 years	Cold PDO phase: 1890–1924, 1947–1976	Warm PDO phase: 1925–1946, 1977–1998
NAO: North Atlantic Oscillation (see Jones et al., 1997; Rivière and Drouard, 2015; Sen and Ogrin, 2016)	Inter-annual and inter-decadal variability of the difference of atmospheric pressure at sea level between the Icelandic low and the Azores High. Inter-annual, and 7.7 years of periodicity	Strongest negative periods: 1962–1963, 1968–1969, 1995–1996, 2009–2010	Strongest positive periods: 1970–1975, 1988–1989, 1994–1995, 2011–2012, 2013–2014
AMM: Atlantic Meridional Mode (see Grossmann and Klotzbach, 2009; Kossin and Vimont, 2007)	Leading mode of basin-wide coupled ocean-atmosphere interaction between SST and low-level winds. Inter-annual and multi-decadal periodicity	Cold AMM phase: 1971–1995	Warm AMM phase: 1925–1970, 1995–2006
AMO: Atlantic Multidecadal Oscillation (see Enfield et al., 2001; Rayner et al., 2003)	Multi-decadal variability in the North Atlantic SST. Periodicity of 50–70 years	Cold AMO phase: 1964–1995	Warm AMO phase: 1926–1964, 1995–present

The Oceanic Niño Index (ONI) is usually used to identify El Niño (warm) and La Niña (cold) years (<http://www.cpc.ncep.noaa.gov/>). ONI is the 3-month running mean of Extended Reconstructed Sea Surface Temperature (ERSST v5) anomalies in the El Niño 3.4 region (<http://ggweather.com/enso/oni.htm>). The El Niño 3.4 anomalies represent the average equatorial SSTs in the equatorial Pacific Ocean (5°N to 5°S latitude, and 120°W to 170°W longitude).

4.4. Crop yield and vegetation

Crop yield data from 1981 to 2015 for quinoa and potato were obtained from the Bolivian National Institute of Statistics (INE, <https://www.ine.gob.bo>) for the administrative regions La Paz, Oruro, and Potosi. The annual crop yield datasets represent production (t) in relation to area (ha) at regional level. No historical crop yield data on local scales are available yet, which is a major limitation for any risk-based approach and need to be addressed in the future. Nevertheless, we suggest that the coarse distribution of the crop yield data can be improved using the NDVI.

Besides improving the crop yield resolution, the NDVI allows to analyse the variability of vegetation at a monthly time scale. This makes it possible to analyse the phenology of the studied crops through to the growth phases. NDVI estimates the vegetation vigour (Ji and Peters, 2003) and crop phenology (Beck et al., 2006). NDVI was assembled from the Advanced Very High Resolution Radiometer (AVHRR) sensors by the Global Inventory Monitoring and Modelling System (GIMMS) at semi-monthly (15 days) time step with a spatial resolution of 0.08°. NDVI 3g.v1 (third generation GIMMS NDVI from AVHRR sensors) and the data set spans from September 1981 to August 2015. Note, that the NDVI is an index that represents a range of values from 0 to 1, bare soil values are closer to 0, while dense vegetation has values close to 1 (Holben, 1986). NDVI 3g.v1 GIMMS provides information to differentiate valid values from possible errors due to snow, cloud, and interpolation. These errors were eliminated from the dataset and replaced with the nearest neighbour value.

The agricultural land in the Bolivian Altiplano was delimited based on the land-use map for Bolivia developed by Raul Lara Rico at the Ministry of Rural Development and Land of Bolivia in 2010 (geo.gob.bo) using Landsat imagery and ground information at a scale 1:1,000,000.

5. Methods

To assess the water scarcity in the Bolivian Altiplano, drought episodes and its drivers were examined (Fig. 5). Firstly, previous research was collected and synthesized, in order to have a state of the art of research with respect to climate and water resources (**Paper I**). Then, analysis of precipitation variability and its association with climate phenomena were made (**Paper II**). After this, the soil moisture was estimated and related to agricultural production (**Paper III**). Finally, the drought risk was assessed to define the association of climate variability with agricultural production (**Paper IV**). The methods used, attempt to assess the water scarcity to support a risk management strategy for the Bolivian Altiplano.

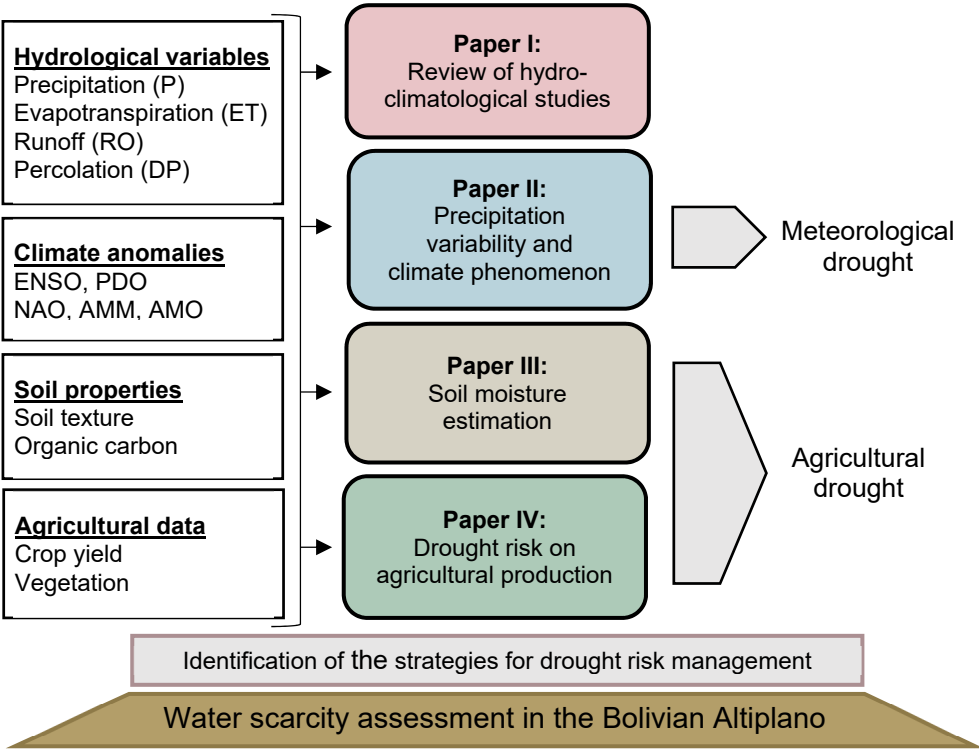


Figure 5. Thesis framework

5.1. Precipitation variability and its relation to climate phenomena

Summer precipitation (DJFM) totals at six locations in the Bolivian Altiplano: Copacabana, El Belen, El Alto, Patacamaya, Oruro, and Potosi Los Pinos were filtered by principal component analysis (PCA) and about 90% of their original variability were kept to reduce noise. PCA was developed by Pearson (1901) and Hotelling (1933). PCA reduces data dimensionality and concentrates variance into a small number of independent variables. After this, maximum covariance analysis (MCA) was applied to the variables. Here, the cross-covariance matrix of the total summer precipitation and averaged climate indices for the same season was investigated. Details of MCA are given by Bretherton et al. (1992) and Wallace et al. (1992). Each MCA mode consists of a pair of singular vectors together with associated time series. The heterogeneous correlation for each MCA mode represents the correlation coefficients between the expansion coefficients for the climate modes and the summer precipitation. Eigenvectors of each mode are orthogonal to other modes in the space domain. Thus, the coupling strength of two fields is represented by the correlation coefficients. Each mode represents a fraction of the totally explained variance. The singular vectors describe the patterns of the fields having a covariance equal to the singular value. Singular values are used to define the squared covariance fraction (SCF) used to compare the relative importance of the expansion of each mode (Bretherton et al., 1992; Rana et al., 2012; Uvo et al., 1997).

Continuous wavelet transform (CWT) was used to analyse non-stationary variability of summer precipitation and climate modes. The climate modes included in the analysis were ENSO, PDO, NAO, AMM, and AMO. Wavelet transform was introduced by Morlet (1983), Grossmann and Morlet (1984), and Goupillaud et al. (1984). The theory of wavelet transform is discussed by Torrence and Compo (1998). The CWT decomposes time series into time-frequency space, enabling the identification of dominant modes of variability and variation in time. For this study Morlet wavelet was used. As the wavelet is not completely localized in time, CWT presents edge artefacts called cone of influence (COI). The COI is the area where the e-folding time of wavelet power drops by a factor e^{-2} . In this study, the circular mean of the phase was quantified for regions statistically significant at 5% and outside the COI. After this, the cross wavelet transform (XWT) was applied for summer precipitation and climate indices. Grinsted et al. (2004) described the theory and application of XWT. The XWT shows regions with high common power between two CWT. XWT can be decomposed into amplitude and phase angles. The phase angles describe the delay between the two signals. And, the phase angles define the phase relationship. The phase arrows point to the right and anti-phase point to the left. The wavelet coherence (WTC) identifies the frequency bands and

time intervals where two time series co-vary (Torrence and Webster, 1999). The WTC represents the coherence of XWT. The significance level of the WTC is defined using Monte Carlo methods, through estimation of significance by an order of 1,000 surrogate data set pairs. The phase angles of the WTC follow the same interpretation as for XWT.

Finally, a band-pass filter using an inverse CWT was applied to reconstruct time series of the climate modes and precipitation for specific band periods of high power spectrum. Here, the analytic Morlet wavelet was used to define the inverse CWT. The reconstructed time series of summer precipitation and climate indices were correlated using spearman correlation to seek statistically significant relationships at 95% confidence level, and the variation of the precipitation explained by the climate indices was defined by the coefficient of determination (square of correlation) between reconstructed series.

5.2. Soil moisture estimations

A soil water balance model was used to estimate the soil moisture at the 6 studied sites (Table 1) from September 1981 to August 2017. In parallel, soil moisture estimations were derived from satellite data. To evaluate the performance of the different datasets, soil moisture estimations was driven by both observed precipitation and satellite top soil water content. The soil moisture estimations were calibrated using gauged soil moisture data from 2013 to 2017. Additionally, relationships between the soil moisture and the crop yield were evaluated.

5.2.1. Soil water balance driven by precipitation

Besides precipitation (P), the variables used for the precipitation driven soil water balance were maximum (TX) and minimum (TN) temperature, wind speed (WS), relative humidity (RH), and solar radiation (SR) from 1981 to 2017. Variable series with less than 10% of missing data, were filled with the mean monthly value of the record. For variables with more than 10% of the data missing, the gaps were replaced with the nearest spatial dataset. The soil moisture was calculated using the soil water balance:

$$\Delta SW_i = I_i + P_i - ET_{c,i} - RO_i - DP_i + CR_i + \Delta SW_{i-1} \quad (1)$$

where ΔSW_i is the soil water content on day i , I is irrigation, P is rainfall, ET_c is crop evapotranspiration, RO is surface runoff, and Pe is percolation. Capillary rise

(*CR*) is the water transported upward from the water table towards the root zone. ΔSW_{i-1} is the soil water content of the previous day.

Irrigation was not considered because only 9% of the cropped surface in Bolivia are irrigated (INE, 2015a). And due to the low capillary rise, this variable was negligible. Hence, the variables soil water content, precipitation, evapotranspiration, runoff, and percolation were considered for the soil water balance:

$$\Delta SW_i = P_i - ET_{c,i} - RO_i - DP_i + \Delta SW_{i-1} \quad (2)$$

The ΔSW was computed on day *i*. The daily precipitation was obtained from gauged data and crop evapotranspiration was deduced using Eq. (3). Runoff occurs when the first soil layer reaches the saturation level. And the percolation is calculated based on the volumetric water content and saturated hydraulic conductivity.

The crop evapotranspiration (Eq. (3), ET_c) is estimated by multiplying the crop coefficient (K_c), the water stress coefficient (K_s), and the reference evapotranspiration (Eq. (4), ET_o). ET_c and ET_o were calculated by the FAO Penman–Monteith equation (Allen et al., 1998). The actual vapour pressure (e_a) was measured based on the temperature at dewpoint T_{dew} . T_{dew} was assumed to be equal to the minimum temperature -3°C based on Garcia et al. (2003):

$$ET_c = K_c K_s ET_o \quad (3)$$

$$ET_o = \frac{0.408 \Delta(R_n - G) + \gamma \left(\frac{900}{T + 273} \right) u_2 (e_s - e_a)}{\Delta + \gamma(1 + 0.34 u_2)} \quad (4)$$

where ET_c is the crop evapotranspiration (mm d^{-1}), K_c is crop coefficient, K_s is water stress coefficient. ET_o is reference evapotranspiration (mm day^{-1}), R_n is net radiation at the soil surface ($\text{MJ m}^{-2} \text{day}^{-1}$), G is soil heat flux density ($\text{MJ m}^{-2} \text{day}^{-1}$), T is mean daily air temperature at 2 m height [$^\circ\text{C}$], u_2 is wind speed at 2 m height [m s^{-1}], e_s is saturation vapour pressure (kPa), e_a is actual vapour pressure (kPa), $e_s - e_a$ is saturation vapour pressure deficit (kPa), Δ is slope for vapour pressure curve ($\text{kPa } ^\circ\text{C}^{-1}$), and γ is psychrometric constant ($\text{kPa } ^\circ\text{C}^{-1}$).

After calculation of ET_o , the evapotranspiration of the quinoa crop was estimated by multiplying ET_o with the crop coefficient (K_c), and the water stress coefficient (K_s , Eq. (3)). The quinoa crop has a growing season length of 150–170 days. The cropping season in the studied area occurs from September to March. Thus, we assumed that quinoa growing season in the studied basin has a duration of 160 days (Geerts et al., 2006). We also assumed that the plant emergence starts when the soil moisture is 60% of the TAW, with the latest day of emergence set to 15th December

(Garcia et al., 2003). The K_c of quinoa under no water stress conditions as reported by Garcia (2003) is 0.52 for the initial stage, 1.0 for the mid-season, and 0.70 at the end of the late season stage. The K_c was adjusted based on actual environmental and soil moisture conditions (Allen et al., 1998). Before the growing season, only soil evaporation was considered. Here, the K_c is equal to the soil evaporation coefficient (K_e), that is the evaporable water of the soil surface layer. Once that the crop has initiated development, the K_c is equal to the K_e in relation with the basal crop coefficient (K_{cb}). For the initial growth stage, the initial K_c depends on the fraction of the wetted soil surface. This fraction is determined by the crop height and precipitation. The K_c for the midseason and late season was adjusted based on the crop height, minimum relative humidity, and mean wind velocity. The minimum relative humidity was measured based on the relation between vapour pressure of the maximum temperature and vapour pressure of the dew-point temperature (T_{dew}).

The effect of limited soil water content to crop needs was included by relating the water stress coefficient (K_s) to the crop evaporation. The water stress only affects the crop transpiration. The K_s was calculated based on the total available water (TAW), the readily available water (RAW), and the actual water content in the soil (SW_i). To define the TAW and RAW, information on field capacity and wilting point are needed. The soil water content at field capacity, wilting point, saturation, and saturated hydraulic conductivity were estimated using soil texture and organic matter content for different layers of the soil (Saxton and Rawls, 2006). Here, field capacity was defined as amount of water that the soil can hold against gravitational forces with a pressure of 33 kPa. Wilting point is the water held to soil particles at a pressure of about 1500 kPa. Plant water extraction was set to 40% of water requirement from the first quarter (top layer) of the root zone, 30% from the second quarter, 20% from the third quarter, and 10% from the fourth quarter (bottom layer) (Ayers and Westcot, 1976), since a greater part of the roots are in the top half of the depth of root zone.

Percolation (Eq. (5)) was calculated following the method described by Savabi and Williams (1995), using the volumetric water content at field capacity (FC), and saturated hydraulic conductivity (K_{sat}). The soil water content exceeding the corresponding field capacity is subject to percolation through the succeeding layer. Water moving below the root zone was considered water loss. During the growing season, we assumed that quinoa presented a root depth of 0.1 m for the initial growing stage, an 0.6 m for the mid- and late stages (Geerts et al., 2006). The unsaturated hydraulic conductivity (K) was calculated for each soil layer. K is defined as the product of K_{sat} with the soil moisture in relation to the saturated Water content.

$$DP_i = 0 \quad \Delta SW_i \leq TAW \quad (5)$$

$$DP_i = (SW_i - FC) \left[1 - e^{-\frac{\Delta t}{t_i}} \right] \quad \Delta SW_i > TAW$$

DP_i is the percolation for day i (mm day⁻¹), SW_i is the soil moisture content (mm day⁻¹), FC is the field capacity water content (mm), Δt is the travel time (day), and t_i is the travel time for percolation (day).

$$t_i = \frac{SW_i - FC}{K} \quad (6)$$

The unsaturated hydraulic conductivity is calculated using:

$$K = K_{sat} \left(\frac{SW_i}{Sat} \right)^B \quad (7)$$

where K_{sat} is the saturated hydraulic conductivity. B is a parameter that causes K to approach zero as SW_i approaches FC . Sat is the saturated water content. The parameter B is defined as:

$$B = \frac{-2.655}{\log \frac{FC}{Sat}} \quad (8)$$

To capture the hydrological dynamics described by these equations, the soil model was evaluated for various calculation steps per day (See Section 5.2.3).

5.2.2. Soil water balance driven by satellite soil moisture

The second method for soil moisture estimation was derived from satellite data. This is the same method as the precipitation driven model for the atmospheric water demand, soil parameters, and percolation dynamics, except that instead of precipitation as input to the water balance, the top soil (50 mm depth from the soil surface) water content was the satellite estimate at the beginning of each day. Top soil water content in excess of field capacity, together with atmospheric water demand, crop transpiration, and percolation dynamics (Eq. (5)), then drove the water availability in each layer of the soil model over the defined calculation steps.

5.2.3. Calibration of the soil water balance model

Given the uncertainties in the soil parameters, observations, model assumptions, and the spatial discrepancy between the satellite grids and observation points, the modelled soil water content was calibrated and fitted to the observed soil water content. Due to a low number of years with observed data (2013–2016), and variation in soil water content between these years, the model was calibrated using the full dataset, with no separate validation conducted at this point. Calibration was done using conductivity rate between layers in the soil model, the number of calculation steps per day, and through linear regressions of the daily soil moisture estimate on the observed daily soil moisture. The conductivity was calibrated by multiplying the saturated hydraulic conductivity with a factor named *K reduction*. *K reduction* was selected based on the best fit to the gauged soil moisture data.

Initial evaluation of the model showed that overestimation of percolation affected the model performance, which justified calibration using parameters related to percolation. Calibration through linear regression gave a good fit for mean and amplitude of modelled data in relation to observations under the set optimization rules (in this case ordinary least squares). Linear regression was opted for over higher order functions to reduce the risk of overfitting, and to retain the original model variation. Calibration of the percolation parameters (conductivity rate, calculation steps) were evaluated for all six regions to select a single set of model parameters with the best overall agreement. To account for regional differences, linear regression was run separately for each region and observation point. Modelled soil moisture was compared as mean value at the given observation depth ± 50 mm.

5.2.4. Soil moisture variability relationship with agriculture

As indicated above, quinoa is a main crop in the Bolivian Altiplano. Therefore, the two soil water models and the resulting crop water use were used to estimate relationships with quinoa yield. To estimate the relationship between crop water use over the growing season and crop yield, seasonal yield reductions were calculated based on water deficit at each growth stage with associated yield reduction factors. For instance, the flowering and grain formation are highly sensitive to water stress, therefore they had larger weight through the yield reduction factors. In contrast, the vegetative stage presents resilience to water stress, thus, it had lower weight. The final seasonal yield reduction was regressed against the crop yield through robust linear regression. Crop yield data were available for the period 1981–2017, and to match this time period for the soil water estimates, climate models were used to derive data for the atmospheric variables, as well as the already presented satellite top soil water estimates.

5.3. Drought risk assessment

Gauged precipitation datasets at 23 stations from the SENAMHI Bolivia were used to validate the CHIRPS satellite rain data (Table 3). The gauged precipitation datasets have less than 10% missing data. Data gaps were filled with mean monthly values from the full dataset. Additionally, gauged temperature at 11 locations was used to validate the monthly mean land surface temperature (LST). The chosen study period was September 1981 to August 2015. The hydrological year in Bolivia is from September to August.

Table 3. Spatial location of gauged precipitation and temperature datasets

Gauged precipitation dataset from 23 locations and 11* gauged maximum and minimum temperature datasets.

N°	Station	Lat	Lon	N°	Station	Lat	Lon
[1]	Achiri*	-17.21	-69.00	[13]	Oruro Aeropuerto*	-17.95	-67.08
[2]	Ancoraimes	-15.90	-68.90	[14]	Patacamaya*	-17.24	-67.92
[3]	Ayo Ayo*	-17.09	-68.01	[15]	Salla	-17.19	-67.62
[4]	Berenguela	-17.29	-69.21	[16]	San Jose Alto*	-17.70	-67.78
[5]	Calacoto*	-17.28	-68.64	[17]	San Juan Huancollo	-16.58	-68.96
[6]	Colcha K	-20.74	-67.66	[18]	San Pablo de Lipez	-21.68	-66.61
[7]	Collana*	-16.90	-68.28	[19]	Santiago de Huata	-16.05	-68.81
[8]	Conchamarca	-17.38	-67.46	[20]	Santiago de Machaca	-17.07	-69.20
[9]	Copacabana	-16.17	-69.09	[21]	Tiahuanacu*	-16.57	-68.68
[10]	El Alto Aeropuerto*	-16.51	-68.20	[22]	Uyuni*	-20.47	-66.83
[11]	El Belen	-16.02	-68.70	[23]	Viacha*	-16.66	-68.28
[12]	Hichucota	-16.18	-68.38				

5.3.1. Validation of satellite data using ground data

The performance of the satellite products was validated using ground data to check if the satellite data accurately estimate rainfall. The validation was based on statistical measures including categorical analyses (e.g., Blacutt et al., 2015; Satgé et al., 2016). The mean error (ME in Eq. (9)), also called bias (Wilks, 2006) shows the degree of over- or underestimation (Duan et al., 2015). Additionally, the Nash-Sutcliffe efficiency (E in Eq. (10)) coefficient evaluates the prediction accuracy compared to observations (Nash and Sutcliffe, 1970). A perfect score corresponds to E equaling one between gauge observation and satellite-based estimate, and zero indicates that the satellite estimations are as accurate as the mean of observed data, and a negative E indicates the observed mean is better than satellite-based estimate. Furthermore, the Spearman rank correlation (Eq. (11)) was computed to estimate the goodness of fit to observations (e.g., Blacutt et al., 2015; Satgé et al., 2016). Correlation coefficients larger or equal to 0.7 were considered reliable (e.g., Condom et al., 2011; Satgé et al., 2016).

$$ME = bias = \frac{1}{n} \sum_{i=1}^n (S_i - G_i) \quad (9)$$

$$E = 1 - \frac{\sum_{i=1}^n (G_i - S_i)^2}{\sum_{i=1}^n (G_i - \bar{G})^2} \quad (10)$$

$$\text{Spearman rank correlation} = \frac{\sum_{i=1}^n (x_i - \bar{x})(y_i - \bar{y})}{\sqrt{\sum_{i=1}^n (x_i - \bar{x})^2 \sum_{i=1}^n (y_i - \bar{y})^2}} \quad (11)$$

For the categorical statistics, the Probability of Detection (POD) and False Alarm Ratio (FAR) were computed. The POD indicates what fraction of the observed events that was correctly estimated, and FAR indicates the fraction of the predicted events that did not occur (Bartholmes et al., 2009; Ochoa et al., 2014; Satgé et al., 2016). The POD and FAR range from 0 to 1, where 1 is a perfect score for POD, and 0 is a perfect score for FAR. Categorical statistic measures were used to evaluate the satellite estimations. Here, the rainfall amounts are considered as discrete values, i.e., rain occurrence or absence. Based on this approach, four scenarios were taken into account: the number of events when the satellite rain estimation and the rain gauge report a rain event (H), when only the satellite reports a rain event but is a false alarm (F), and when only the rain gauge reports a rain event but not the satellite not and therefore is a miss (M).

5.3.2. Crop yield simulation based on NDVI data

For this study NDVI was related with quinoa and potato yields from 1981 to 2015. The association between quinoa and potato yield and NDVI was developed using Spearman's rank correlation for the agricultural land area of the Bolivian Altiplano. The maximum semi-monthly NDVI of March and April for every year was identified. March and April generally represent the period of maximum phenological development of quinoa and potato crops in the Altiplano. The maximum NDVI of each grid was compared to the annual crop yield at La Paz, Oruro, and Potosi. The NDVI grids and crop yield correlations equal or larger than 0.6 (Spearman correlation, $p = 0.05$) were considered as adequate for crop yield estimation (e.g., Huang et al., 2014a). Then, a regression approach was applied for selected NDVI grids and corresponding precipitation and temperature.

5.3.3. Regression of vegetation and climate variables

Only NDVI grids that properly simulated the crop yield were related to climate variables (Spearman correlation larger than 0.6). For this, stepwise regression was applied to quantify the effect on vegetation as a function of precipitation and temperature variance (Eq. (12)). The stepwise regression combines forward selection and backward elimination technique to increase the robustness of the results. The NDVI was set as independent variable, and for the same spatial location the dependent variables were accumulated precipitation and accumulated degree days (ADD). Firstly, the NDVI was related only to satellite precipitation. Subsequently, accumulated precipitation and ADD were related to vegetation.

For the forward selection, variables were entered into the model one at a time in an order determined by the strength of their correlation with the criterion variable (only including variables if they were significant on the 5% level). The effect of adding each variable was assessed during its entering stage, and variables that did not significantly add to the fit of the model were excluded (Kutner et al., 2004). For backward selection, all predictor variables were entered into the model first. The weakest predictor variable was then removed and the regression fit re-calculated. If this significantly weakened the model then the predictor variable was re-entered, otherwise it was deleted. This procedure was repeated until only useful predictor variables (in a statistical sense, e.g., significant as well as model fit) remained in the model (Rencher, 1995). The results were compared with other results from the literature to check for suitability of results with phenology and weather related dimensions of plants.

$$NDVI = \beta_0 + \beta_1 \text{accumulated precipitation} + \beta_2 ADD \quad (12)$$

Both precipitation and temperature were represented as accumulated data. To calculate the ADD, the accumulated value of the Growing Degree Day (GDD) multiplied by the number of days of each month was computed. The GDD is defined as the difference between mean and base temperature. The mean temperature (T_{mean}) is the arithmetic average between maximum and minimum temperature, and the base temperature (T_b) is the minimum threshold for the plant development. T_b of potato was 4°C and 3°C for quinoa (Jacobsen and Bach, 1998). If T_b is greater than T_{mean} , the GDD is equal to 0. Only the period of growing season was considered for the ADD calculation. The growing season of quinoa is from September to April, and for potato it is October to April.

The cumulative precipitation was calculated for a period of 12 months from September to August of the following year for all locations. It should be noted that the precipitation in the Altiplano shows a marked rainy season from November to March. The peak of precipitation is in December and January. And, NDVI displays

the highest peak in March and April. The lag between the max precipitation and max NDVI is reasonable since vegetation requires time to grow (e.g., Chuai et al., 2013; Cui and Shi, 2010; Shinoda, 1995). For this reason, the regression of NDVI and accumulated precipitation and ADD were developed considering a lag of two, three, and four months for the agricultural area.

5.3.4. Crop yield relationship with ENSO

The Oceanic Niño Index (ONI) was used to identify El Niño and La Niña years. Five consecutive overlapping three-month periods at or above +0.5°C anomaly represent warm events (El Niño), and at or below the -0.5 anomaly cold (La Niña) events. This threshold was further broken down into weak (with a 0.5 to 0.9 SST anomaly), moderate (1.0 to 1.4), and strong (≥ 1.5) events. In our study we considered the categories neutral/moderate (with a -1.4 to 1.4 SST), strong El Niño (≥ 1.5) and strong La Niña (≤ -1.5) years (Table 4). The classification considered three consecutive overlapping 3-month periods at or above the +1.5°C anomaly for warm (El Niño) events and at or below the -1.5°C anomaly for cold (La Niña) events. The ENSO year in this study starts in September-October-November and ends in August-September-October for each year from 1981 to 2015. Subsequently, the crop yield of quinoa and potato was compared with strong El Niño years. This relationship was analyzed using parametric two sample t-test as well as the non-parametric Wilcoxon rank sum test. In more detail, the two sample t-test and Wilcoxon rank sum compare two independent data samples, with the difference that the first compares samples that assume a normal distribution, and the second is a non-parametric test which is based on the ranking of empirical values (Wilks, 2006). The null hypothesis of the two sample t-test was that crop yields during El Niño and neutral/moderate years have equal means. The null hypothesis of the Wilcoxon rank sum test was that the crop yield during El Niño and neutral/moderate years are samples from continuous distributions with equal median. Both tests compute two-sided p-value. When the hypothesis is equal to 1, the null hypothesis is rejected at 5% significance level. And the null hypothesis is accepted when it is equal to zero.

Table 4. Classification of ENSO

Strong El Niño (≥ 1.5 °C), strong La Niña (≤ -1.5 °C) and neutral/moderate (-1.4 to 1.4 °C) years for the time period 1981 to 2015.

Strong El Niño	Neutral and moderate	Strong La Niña
1982–83	1981	1988–89
1986–87	1984–1985	1998–99
1987–88	1989–1990	2007–08
1991–92	1992–1996	2010–11
1997–98	2000–2006	
	2008–2009	
	2011–2014	

6. Results and discussion

The rainy season in the Bolivian Altiplano occurs during austral summer months (Garreaud et al., 2003; Vuille and Keimig, 2004). Monthly total precipitation is shown for the northern, central and southern Bolivian Altiplano in Fig. 6. Larger amount of annual precipitation is recorded for the northern Altiplano (Fig. 6a). From September to August of the following year is considered the hydrological year in the studied region. Here, the mean annual precipitation is about 800 mm. In contrast, the mean annual precipitation in central Altiplano is about 400 mm, and in the Southern Altiplano about 200 mm. The annual precipitation is more distributed in the northern Altiplano. December, January and February are the wettest months. The peak is more noticeable in the southwest Altiplano (Fig. 6c). The summer months (DJFM) concentrate about 70% of the total precipitation in northern and 80% in the southern Altiplano.

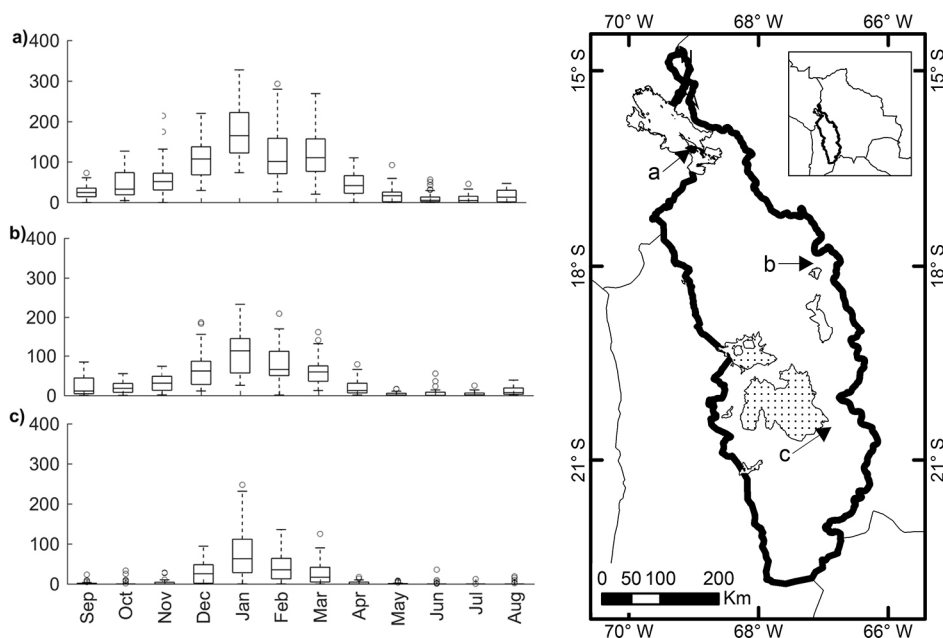


Figure 6. Boxplots of monthly precipitation
Total monthly precipitation in the northern, central, and southern Bolivian Altiplano from 1980 to 2016 at (a) Copacabana station, (b) Oruro station, and (c) Uyuni station.

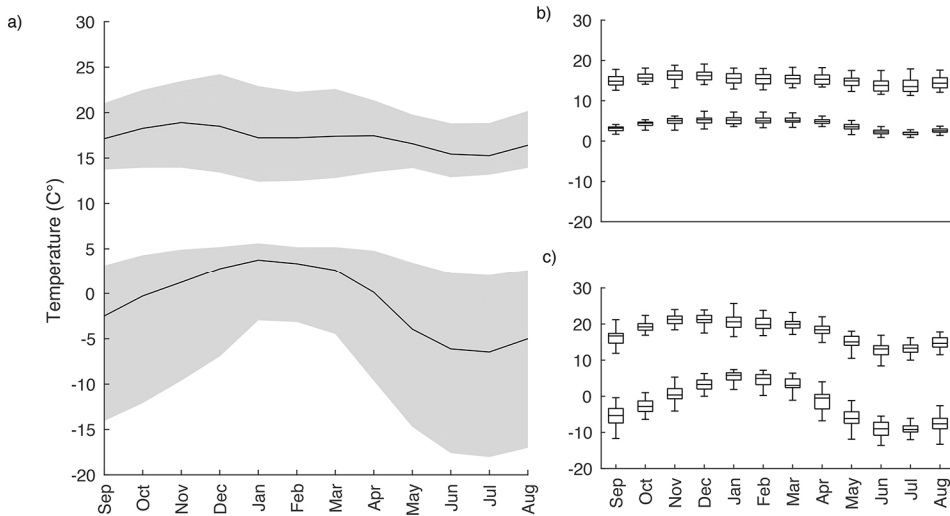


Figure 7. Mean monthly maximum and minimum temperature

(a) Average of mean monthly maximum and mean monthly minimum temperature of 11 datasets in the Bolivian Altiplano from 1981 to 2016 (black solid line). The range of the monthly temperature (shaded area). Boxplot of the monthly maximum and minimum temperature in (b) Copacabana station and (c) Uyuni station, respectively.

Temperature in the Altiplano represents annual and inter-annual variance. Maximum monthly temperature occurs in November and March (Fig. 7a). This is due to the higher radiation during summer months. However, the heat is neutralized by clouds from December to February. Minimum temperature presents larger variability than the maximum, with an evident peak during summer months. This variation is more noticeable in the southern Altiplano (Fig. 7c). Here, minimum temperature over 0°C during summer and about -10°C during winter occur. In contrast, the northern Altiplano shows lower variation during the year (Fig. 7b). Here, the maximum temperature is above 10°C and minimum temperature is above 0°C all along the year.

6.1. Precipitation variability

Heterogeneous correlation results from the MCA show that 77% of the total variance are explained by the first two modes. The first mode explains 51% and the second mode 26% of the total variance. The squared covariance factor (SCF) for the first mode represents 74%. This mode is characterized by Niño3.4, Niño3, and NAO, negatively correlated with summer precipitation at all stations. This confirms previous research findings that ENSO and precipitation are negatively related in the Altiplano (Garreaud, 2009; Thibeault et al., 2012). On the other hand, ENSO presents a dynamic teleconnection with NAO (Huang et al., 1998; Li and Lau,

2012). This teleconnection suggests a similar response to precipitation. This could explain the lower precipitation found during positive phases of ENSO and NAO.

The second mode (explaining 26% of total variance) has a SCF of 19%. Significant negative correlation between precipitation at Potosi Los Pinos and PDO is present. The ENSO and PDO have similar influence on precipitation variability (Andreoli and Kayano, 2005). This explains the negative correlation for the Potosi Los Pinos. The second mode also shows a positive relationship between precipitation in Potosi Los Pinos and AMO. This indicates larger precipitation occurrence during positive phases of the AMO. However, previous studies indicate a relation between the AMO positive phase and the northwards displacement of the ITCZ (Kossin and Vimont, 2007). The ITCZ shift northwards should produce a reduction of the tropical summer precipitation (Flantua et al., 2016). Thus, a separate analysis of the relationship between seasonal precipitation and AMO was needed to evaluate these results. Here, we used wavelet analysis for precipitation and climate indices.

6.1.1. Wavelet analysis

The CWT of summer precipitation shows significant power around the 1980s for all studied regions (Fig. 8). Significant power is also shown during mid-1990s until 2000 for Copacabana and El Belen. During the 1960s, statistically significant power is noticeable especially for Potosi Los Pinos. Statistically significant wavelet power is present for the band $\sim 2\text{--}8$ years. El Alto and Oruro show high power for the band $\sim 10\text{--}15$ years, but only significant in El Alto. Patacamaya shows significant power periods of $\sim 16\text{--}20$ years. But, most of the power is inside the COI except in 1980.

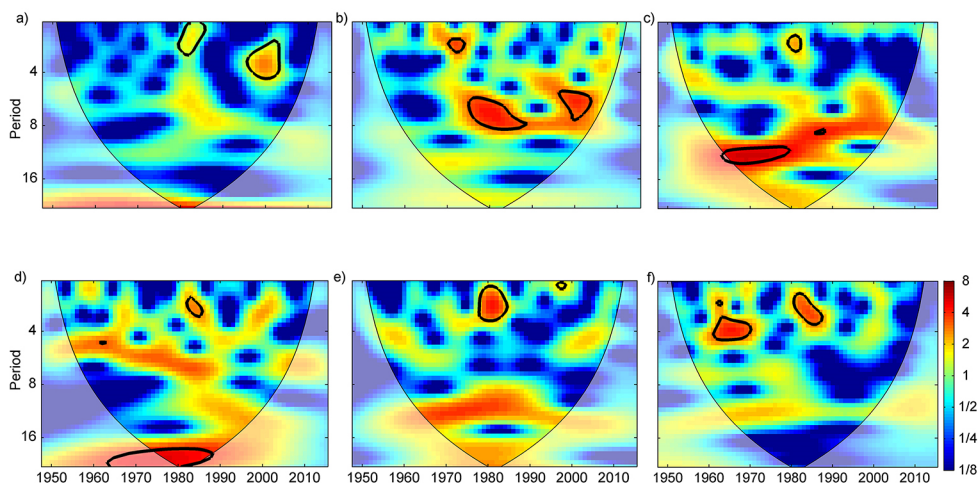


Figure 8. Cross Wavelet Transform (CWT) for summer precipitation
CWT for (a) Copacabana, (b) El Belen, (c) El Alto, (d) Patacamaya, (e) Oruro, and (f) Potosi Los Pinos. The thick contour designates the 5% significance level. The COI is shown in lighter shade. From Canedo-Rosso et al. (2019b).

Figure 9 shows the CWT results for climate modes. The CWT for Niño3.4 and Niño3 represents statistically significant power for a band $\sim 2\text{--}7$ years. The time periods when Niño3.4 shows a significant variance coincide with El Niño and La Niña events. For instance, 1982–1983 and 1997–1998 show significant power, and strong El Niño events were documented (e.g., NOAA Climate Prediction Center). The PDO displays high power for band $\sim 16\text{--}20$ years, but most of this is not significant and it is inside the COI. In contrast, NAO high power is shown for the band $\sim 6\text{--}8$ years during the period 1960 to mid-1980s. Previous research also found that NAO highest power is shown in a periodicity of about 7.7 years (Feliks et al., 2010; Gámiz-Fortis et al., 2002; Paluš and Novotná, 2011; Rogers, 1984; Sen and Ogrin, 2016). NAO shows statistically significant power in the band ~ 4 years at about 2010, but most of the power is inside the COI. The CWT for the AMM shows statistically significant power for bands of 2 and 10–13 years, during the period 1970s to mid-1980s. Finally, AMO shows relatively high power for the band ~ 20 years, but most of this is inside the COI. The AMO has an oscillation of 65–70 years (Schlesinger and Ramankutty, 1994). However, that band period is inside the COI, where edge effects cannot be ignored, and therefore the results in this area are unreliable.

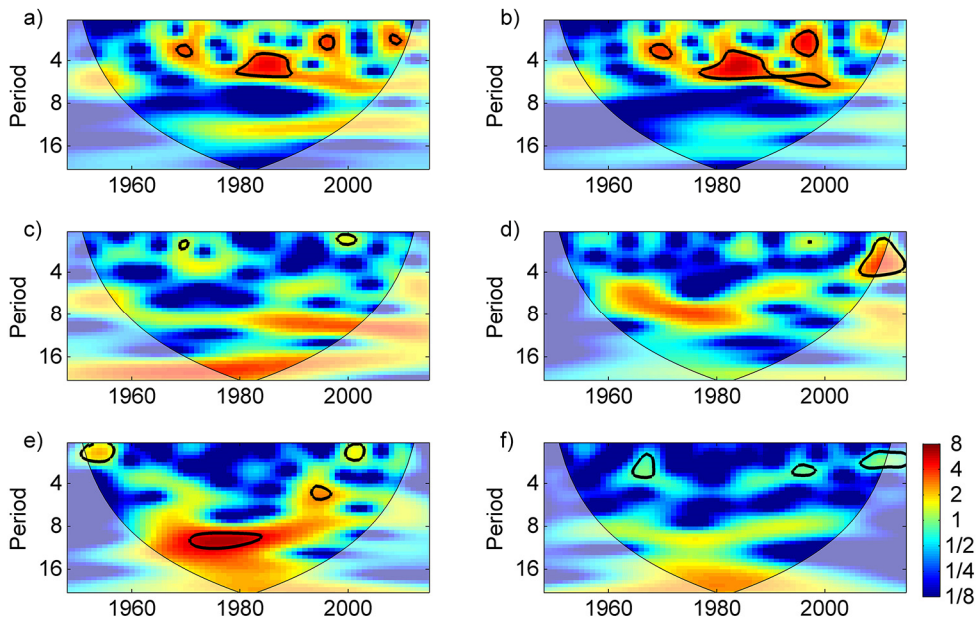


Figure 9. Cross Wavelet Transform (CWT) for climate modes
 CWT for (a) the Niño3.4, (b) the Niño3, (c) PDO, (d) NAO, (e) AMM, and (f) AMO. The thick contour designates the 5% significance level. The COI is shown in lighter shade.

The XWT was applied to find periods where climate indices and precipitation present common power, and it was compared with the WTC to quantify the local correlation of the time series. The XWT of Niño3.4 and summer precipitation show statistical significance for power during $\sim 2\text{--}5$ years for all the stations. The XWT results of Niño3 and summer precipitation are similar. The XWT shows significant common power in the band period $\sim 5\text{--}7$ years for El Belen, El Alto, and Patacamaya. The XWT phase angle pointing to the left suggests that ENSO (Niño3.4 and Niño3) and precipitation are in anti-phase. However, the large standard deviation mainly for Patacamaya and Potosi Los Pinos indicates influence from other climate factors. Similar to the XWT, the WTC for the ENSO and precipitation shows statistically significant correlation for all locations, with arrows pointing to the left suggesting an anti-phase. In contrast, the results of XWT of NAO and precipitation show high common power for the band $\sim 5\text{--}8$ years. During the 1960s, significant common power is shown for Patacamaya in the XWT results, and for El Alto, Patacamaya, and Oruro in the WTC results. From mid-1970s to mid-1980s, high power is shown for the XWT for El Belen, El Alto, Oruro, and Potosi Los Pinos. But only El Belen shows significant power. For that periodicity, the WTC shows statistically significant correlation for Los Pinos. The arrows pointing to the left for the XWT and WTC suggest an antiphase relationship between the NAO and summer precipitation.

The XWT of the AMM and summer precipitation present statistical significant power in the band $\sim 8\text{--}13$ years for all stations except Copacabana. The WTC at this band is statistically significant, except for Patacamaya. The XWT for the AMM and precipitation mean phase evidence of an antiphase relationship indicated by arrows pointing left. Whereas, the XWT for the AMO and precipitation shows high power for the band $\sim 8\text{--}13$ years, only significant for El Alto, where the mean phase angle indicates an antiphase relationship with the arrows pointing left. The power for the XWT and WTC for the band $\sim 16\text{--}22$ years is inside the COI, here the results are unreliable. Despite a positive relationship between AMO and Potosi Los Pinos for the MCA, the XWT for the band $\sim 8\text{--}16$ years presents arrows pointing to the left, suggesting an antiphase relationship. But, the arrows for the band $\sim 2\text{--}4$ years are pointing to the right, suggesting a positive relationship. In any case, the similarity between the patterns for this period is low and might be a coincidence. It is important to point out that AMM and AMO are related to an anomalous meridional SST gradient in the tropics, and a shift of the ITCZ location (Vimont and Kossin, 2007). The summer precipitation in the Altiplano is strongly negatively correlated with the AMM on decadal time scales, but this relation was not significant for AMO. Further analysis is needed to identify the physical mechanisms of the AMO variations.

6.1.2. Band-pass filter reconstruction

A band-pass filter reconstruction for the time series was defined using the inverse of the CWT. Niño3.4 and Niño3 time series were reconstructed for the band period ~2–7 years. The results show significant negative correlation for all the stations (except for Niño3.4 and El Belen). The results confirm that ENSO has a negative relationship with precipitation in the Altiplano. Also, the coefficient of determination (R^2) suggests that the Niño3 explains from 10 to 33% of the precipitation variance. On the other hand, the time lapse reconstruction for NAO and summer precipitation was applied for the band ~5–8 years. NAO presents a negative relationship with precipitation. This negative relationship is significant for El Belen, El Alto, Oruro, and Potosi Los Pinos. And, the R^2 for these time series suggest the precipitation variance is explained from 10 to 29% by the NAO. Furthermore, the reconstructed time series of AMM and summer precipitation were defined for the band ~10–13 years. The correlation between AMM and precipitation are significant for Copacabana, El Alto, and Oruro. With a R^2 equal to 7, 16, and 18% respectively. During positive AMM the ITCZ is displaced northwards (Kossin et al., 2010). Thus, drier conditions are likely to occur in the Altiplano. The Atlantic modes are important, due to their influence on the humid air transport from the Amazon to the Altiplano during the summer (e.g., Garreaud and Aceituno, 2001).

6.2. Soil water estimations

Figure 10 shows the monthly observed precipitation, gauged, and satellite soil moisture for the top soil of Tambillo. Precipitation is concentrated to summer months leading to higher soil moisture. The gauged soil moisture during winter months (JJA) is close to wilting point (6%), and during summer months (DJF) close to or above field capacity (15%). In 2014, the soil moisture is close to saturation (38%). The satellite soil moisture also presents an oscillation with a peak during summer months, however, it shows an overestimation compared to gauged data. The Spearman rank correlation shows significant correlation coefficients at daily and monthly time-step between gauged and satellite soil moisture for the top soil layer (Table 5). For this, we assumed that satellite data can estimate the soil moisture if the bias is corrected using the gauged data. No satellite data of soil moisture are available for Viacha and Puchukollo.

Table 5. Gauged and satellite soil moisture correlation
Correlation coefficient (r) between gauged and satellite soil moisture top soil layer at 0.001 significance level.

Study region	r for daily data	r for monthly data	Gauged SW depth (mm)
Tambillo	0.69	0.82	50
San Gabriel	0.62	0.65	250
AltoLima	0.63	0.74	300
Brabol	0.63	0.73	250

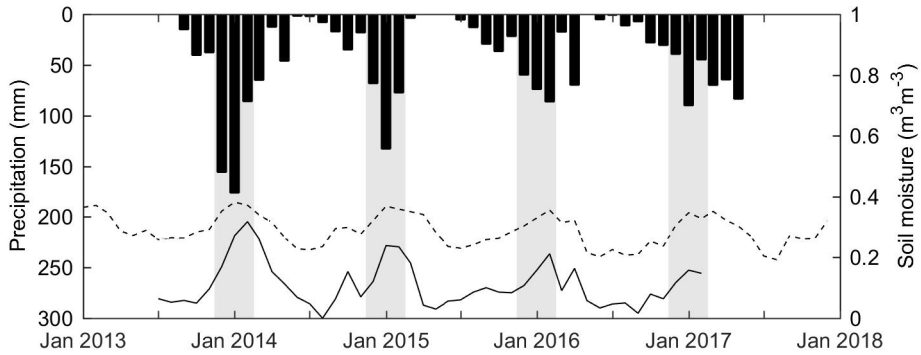


Figure 10. Precipitation and soil moisture

Monthly precipitation (left axis) and mean monthly soil moisture (inverse right axis). Gauged (solid line) and satellite soil moisture (dashed line) data for Tambillo. The shaded areas represent the summer months DJF.

6.2.1. Soil water balance calibration

For the calibration results, the highest linear correlation is shown for K reduction equal to 0.1, that resulted in best agreement between modelled and observed soil moisture for both precipitation and satellite driven models. Considerable differences are, however, seen between the regions and the two soil moisture models. This indicates a large variation in soil parameters between the regions, high influence from the driving dataset, and an incomplete model specification. Similarly, the lowest number of calculation steps per day (5 steps) generally had the highest performance. This indicates that the percolation dynamics as described by the governing equations in Section 5.2.1 overestimate the actual percolation for the specific conditions in these regions. Selection of the smallest number of calculation steps further shows that the model output diverges from the observations with additional model complexity, and conversely that a simpler model is more appropriate in this case.

6.2.2. Soil moisture estimations

Figure 11 (left) shows the results of the calibrated soil moisture estimations driven by satellite soil moisture at 50 and 200 mm of soil depth. Here, the linear regression between gauged soil moisture and the calibrated soil moisture estimation shows a coefficient of determination of 0.65 and 0.71 for a soil depth of 50 and 200 mm, respectively. Only Tambillo presents gauged data at 50 mm. Here, the daily variability is more noticeable. And, the soil moisture shows a peak during the summer (January and February). The calibrated soil moisture estimation driven by precipitation is also shown in Fig. 11 (right). Here, the correlation coefficient between gauged data and the calibrated soil moisture is 0.41 and 0.52 for a soil depth of 50 and 200 mm, respectively.

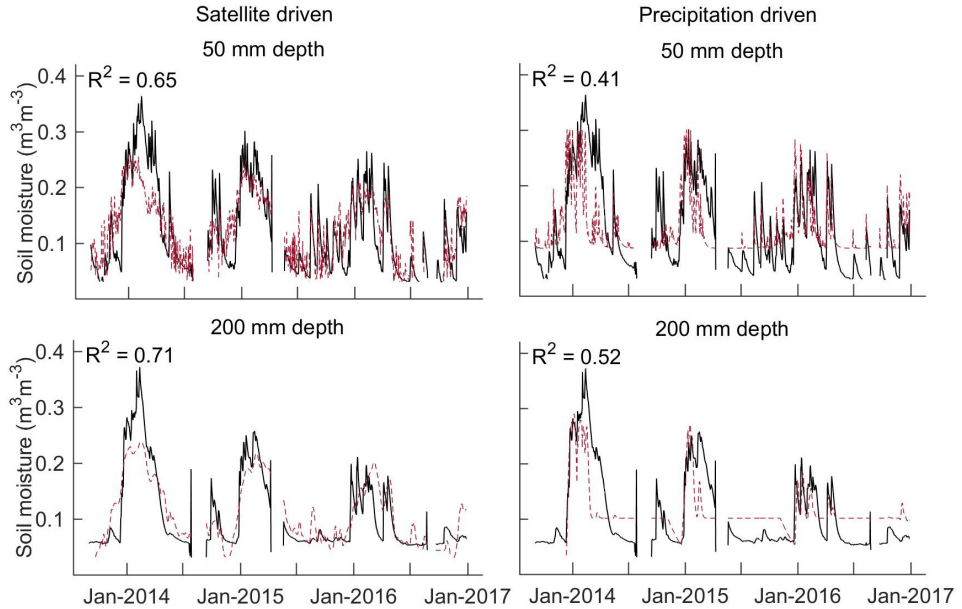


Figure 11. Calibrated soil moisture estimations

The daily soil moisture estimation is denoted by a dashed red line, and the gauged soil moisture is denoted by a solid black line for Tambillo.

San Gabriel, Viacha-IBTEN Alto Lima, Brabol and Puchukollo present gauged data for the soil layer from 250 to 300 mm. Here, the coefficient of determination between gauged soil moisture and soil moisture driven by precipitation (satellite data) San Gabriel 0.18 (0.27), Viacha-IBTEN 0.21 (no satellite data), Alto Lima 0.16 (0.06), Brabol 0.19 (0.19), and Puchukollo 0.11 (no satellite data). Finally, the coefficient of determination between gauged soil moisture and soil moisture driven by precipitation and satellite data for the soil layer depth between 700 to 800 mm is close to 0 for all the stations.

Only the soil moisture estimations for Tambillo are acceptable. This could be due to two reasons. First, the gauged soil moisture is measured at 50 mm soil depth, and this gives important information for the calibration process. Second, the soil moisture at Tambillo varies according to the summer rainy season, showing a peak in January and February. This variation is shown for the soil moisture at 50 and 200 mm of soil depth. In the Bolivian Altiplano, it is expected that the soil moisture is larger during the rainy season, and lower during the dry season. This pattern is not noticeable for the other studied regions.

6.3. Drought risk assessment

6.3.1. Validation of satellite imagery using gauged data

Validation of the CHIRPS satellite rain data was defined using gauged precipitation datasets at 23 locations in the Bolivian Altiplano (Table 3, Fig. 12). Significant correlations were found for all regions ($P < 0.001$). The coefficients were higher than 0.7 except for Colcha K [6], with a correlation of 0.66. The datasets from the airports in Bolivia have a better data quality (e.g., Hunziker et al., 2018). And CHIRPS gives the best fits for the datasets at the airports (El Alto Aeropuerto [10] and Oruro Aeropuerto [13], with coefficients larger than 0.9). The ME (bias) between satellite and gauged data showed a range from -25 to 25% for all datasets, except for San Pablo de Lipez [18], that had a bias of -29%. Previous studies indicate that a bias from -25 to 25% represents a satisfactory fit (see Moriasi et al., 2007). Other studies included a bias from -30 to 30% as satisfactory fit (see Shrestha et al., 2017). In conclusion, the CHIRPS shows a good performance compared with gauged data.

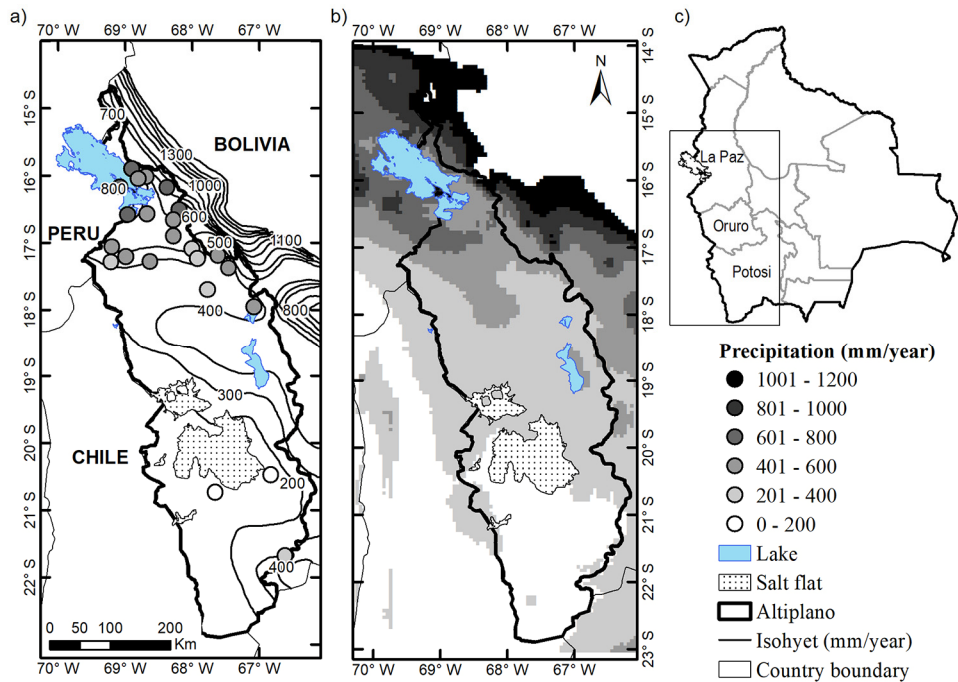


Figure 12. Gauged and CHIRPS satellite-based precipitation

Mean annual precipitation from September 1981 to August 2015 for (a) 23 precipitation gauges (circles), isohyets (solid line), for (b) CHIRPS satellite rainfall product and (c) Bolivia, and the major administrative divisions: La Paz, Oruro and Potosi, where crop yield data are available in the Altiplano. From Canedo-Rosso et al. (2019a).

The Nash-Sutcliffe efficiency coefficient (E) was larger than 0.5 for all stations except Berenguela [4] with a coefficient of 0.43. As a consequence, the E coefficient showed that the mean square error is lower than the variance of the gauged data for all stations, including Berenguela [4]. Moreover, Achiri [1], Colcha K [6], El Alto Aeropuerto [10], Oruro Aeropuerto [13], Patacamaya [14], and Salla [15] presented an E larger than 0.75. This means that there was a very good fit between CHIRPS and gauged precipitation, and the rest had a good fit except for Berenguela [4] (see Moriasi et al., 2007).

6.3.2. Regression of NDVI and climate variables

The precipitation season occurs during austral summer (DJFM) with a peak in January and February (Fig. 13a). The vegetation development shows a maximum during March-April. The NDVI (Fig. 13b) shows a similar growing pattern as the crop phenology (September-April). The minimum temperature shows larger variability. The higher temperature during the austral summer (Fig. 13a) could lead to higher evapotranspiration. With this presumption, we analysed the relationship between NDVI and climate variables: precipitation and temperature. In a first step, the relationship between the maximum NDVI of March-April and the corresponding annual crop yield was defined. A total of 26 and 76 NDVI grids of quinoa and potato yield, respectively, provided satisfactory estimates. Here, a threshold for acceptable performance was a spearman correlation coefficient ($p < 0.05$) larger than 0.6 (see Huang et al., 2014a).

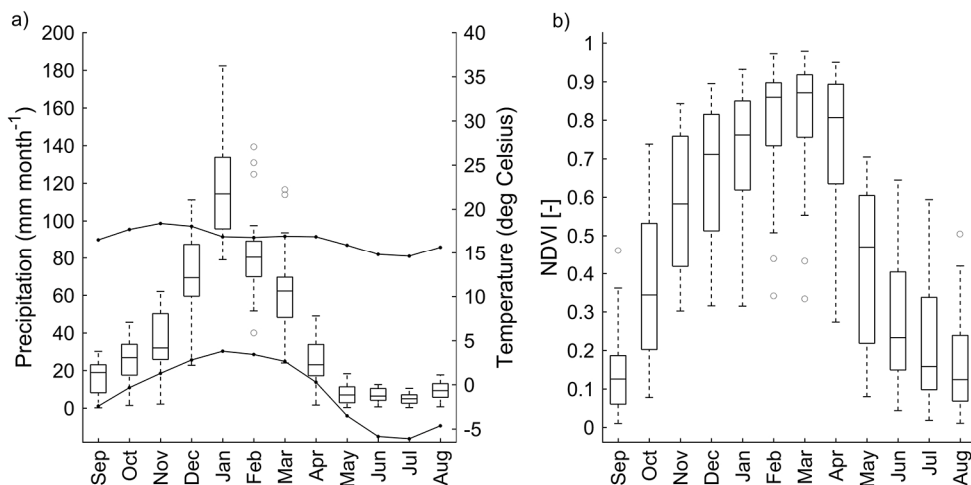
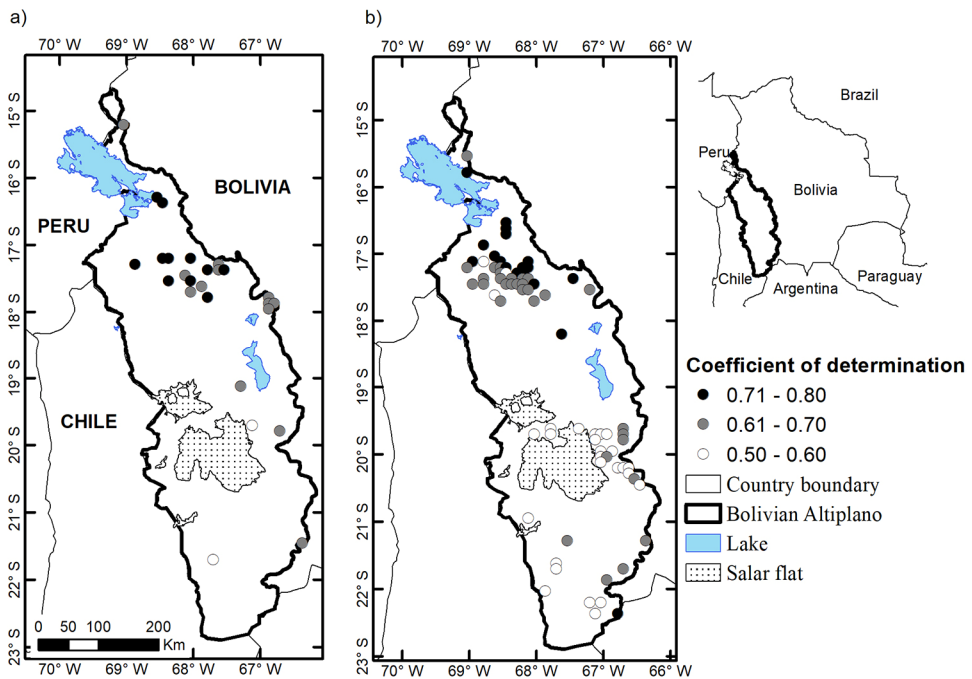


Figure 13. Monthly vegetation index and total precipitation
 (a) Boxplots of mean monthly precipitation and average maximum and minimum temperature (solid line) from September 1981 to August 2015 for the 23 gauged stations. (b) Mean monthly NDVI at the same spatial locations. From Canedo-Rosso et al. (2019a).

Stepwise linear regression was tested using selected NDVI grids and accumulated CHIRPS rainfall datasets at the same spatial location with a lag of two, three, and four months that were statistically significant at 0.01 level. The coefficient of determination (R^2) oscillated from 0.4 to 0.7. Additionally, stepwise linear regression for NDVI as independent variable, and the accumulated precipitation and ADD as dependant variables was performed (Eq. (12)). The results showed statistical significance for all studied locations. The R^2 oscillated from 0.5 to 0.8 for a lag of 4 months (Fig. 14). It should be noted that the R^2 is generally larger in the northern and central Bolivian Altiplano ($R^2 > 0.6$), where the total precipitation is larger. This indicates that precipitation and temperature explain most of the variability of the crop yield, and the influence is more notable in the northern and central Bolivian Altiplano. Despite the large dependence to climate factors, the agricultural production is also affected by other factors in the in Altiplano. For instance, agriculture is affected by the low water retention ability of the soil in the Altiplano (Garcia et al., 2007). In the southern Altiplano sandy and rocky soil prevails, strong winds, and intense solar radiation exist due to the high altitude (Winkel et al., 2015). This condition increases the water loss through infiltration and evaporation.



Regression models with only precipitation as dependent variable showed a larger coefficient of determination for a lag of three and four months. In northern and central Bolivian Altiplano (16 to 19 ° S) larger R^2 was found with a three-month lag and in the southern Bolivian Altiplano (20 to 22° S) with a 4-month lag. The regression with precipitation and temperature as dependent variables showed larger coefficients of determination for a 4-month lag. The results are related to different sowing time and starting period of the rainy season in the area. In the northern Bolivian Altiplano, the rainy season lasts longer than in the southern Altiplano. In the southern Altiplano, the rainy season is mainly concentrated from December to February. The water availability in the soil and the hours of sun required for crop development can explain the lag between the relation of vegetation growth and climate variables.

6.3.3. Relationship between ENSO and crop yield

The relationship between ENSO and crop yield was analysed using two sample t-test and Wilcoxon Rank-Sum Tests for La Paz, Oruro, and Potosi. To test the relationship, crop yield during neutral/moderate years was compared with crop yield during El Niño years (see Table 4). The results showed that quinoa yield during strong El Niño and neutral/moderate years represents a significant difference at 95% confidence level except for Oruro (Fig. 15a). The yield during neutral/moderate years is higher with about 0.2 t/ha compared to El Niño years in La Paz and Potosi.

In Oruro, quinoa yield production during strong El Niño years is lower than the mean yield for neutral/moderate years in most of the cases with an exception in 1982–1983 (Fig. 15a). This finding contradicts previous studies that reported large agricultural losses during 1982–1983 and 1997–1998 (Santos, 2006). On the other hand, the quinoa yield has constantly increased during the last years, mainly in Oruro. This could be explained by employment of advanced crop management strategies (e.g., selected crop varieties and application of agricultural innovations), as this region is one of the largest producer in Bolivia and the world (Ormachea and Ramirez, 2013). Despite the quinoa's high tolerance to environmental stress including drought (Jacobsen et al., 2005; Jacobsen et al., 2003), larger losses are evident mainly during El Niño years. This may be due to the crop's sensitivity to water stress during specific stages of the growing season, and the most sensitive stages are the emergence, flowering, and grain development (see Geerts et al., 2008a; Geerts et al., 2009). The risk for crop yield reduction could be reduced here with irrigation during the sensitive phases of the quinoa crop development. A strategy like deficit irrigation could be employed (Geerts et al., 2008b; Talebnejad and Sepaskhah, 2015). Another strategy to mitigate the crop yield reduction is implementation of crop varieties more resistant to water stress (e.g., Sun et al., 2014).

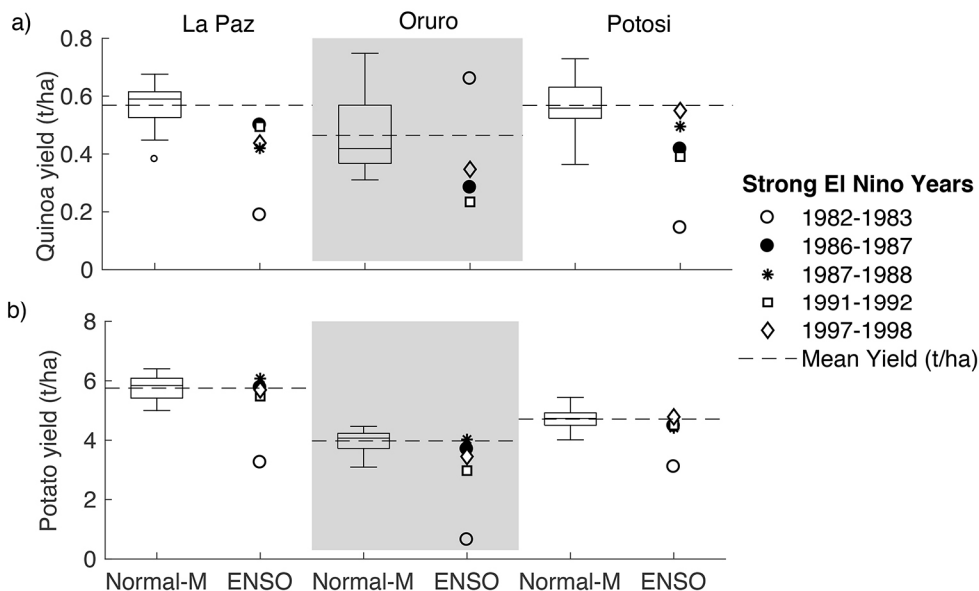


Figure 15. Crop yield during normal/moderate and ENSO years

The boxplot of (a) quinoa and (b) potato yield for normal and moderate (Normal-M) years for La Paz, Oruro, and Potosi. Crop yield during strong El Niño years (markers). Mean of crop yield during normal and moderate years (dashed line). From Canedo-Rosso et al. (2019a).

The t-test and Rank-Sum test results showed that potato yield during neutral/moderate and El Niño years is significantly different at 95% confidence level except for La Paz. The results showed that production during neutral/moderate years is higher in Oruro and Potosi (Fig. 15b). All regions showed lowest potato yield during strong El Niño 1982–1983, with a yield reduction of 40, 80, and 30%, as compared to mean yield during normal/moderate years in La Paz Oruro and Potosi, respectively. The yield reduction during other El Niño events seems to have a larger effect in Oruro. Besides, El Niño events during 1982–1983, potato yield in La Paz showed lower vulnerability to this phenomenon. This could be explained by closeness to the Lake Titicaca and other water bodies that might be used as a water source during precipitation deficit. Similar strategies for drought mitigation (e.g., irrigation and resistant crop varieties) could be implemented in order to avoid large crop losses. However, knowing that a very strong El Niño could lead to large agricultural losses, insurance policy could be assigned to farmers in order to manage the risk before the occurrence of a drought event. For the implementation of any drought mitigation strategy, identification, evaluation, and monitoring of drought risk are crucial. Especially important is our findings that ENSO must be taken explicitly into account in such considerations.

7. Summary and conclusions

The assessment of water scarcity in the Bolivian Altiplano was analysed using a meteorological, hydrological, and agricultural approach. Firstly, the precipitation variability was analysed in relation with climate anomalies for six locations in the Altiplano: Copacabana, El Belen, El Alto, Patacamaya, Oruro, and Potosi Los Pinos. Here, the total summer precipitation (DJFM) from 1948 to 2016 was related to El Niño-Southern Oscillation (ENSO: Niño3.4 and Niño3), Pacific Decadal Oscillation (PDO), North Atlantic Oscillation (NAO), Antarctic Meridional Mode (AMM), and Atlantic Multi-decadal Oscillation (AMO). A statistically significant correlation between climate indices and precipitation was found. The cross wavelet analysis (XWT) permitted to identify a significant power spectrum of the signal. The results were used to define a band-pass filter to represent the signal at higher frequency. For the Niño3.4 and Niño3, the band-pass filter was applied at band ~2–7 years, for NAO at band ~5–8 years, and for AMM at band ~10–13 years. Here, a negative correlation was identified between precipitation and ENSO, NAO, and AMM. This means that less precipitation generally occurs during the positive phase of the mentioned modes. Previous studies confirm the association of drier conditions during ENSO positive phases in the Bolivian Altiplano (Garreaud et al., 2003; Garreaud and Aceituno, 2001; Thibeault et al., 2012). We also know that ENSO and NAO are dynamically linked through teleconnections (Huang et al., 1998; Li and Lau, 2012). Hence, a similar response is shown in association with the summer precipitation variability. And, AMM positive phases represent drier conditions in the studied area (Flantua et al., 2016) due to the northward shift of the ITCZ (Kossin and Vimont, 2007). This knowledge can be used to improve forecasting of seasonal precipitation.

The soil moisture was estimated using two methods, first the implementation of the soil water balance and second the estimation derived from satellite data product for the Katari River basin located in the Bolivian Altiplano. This part of the study aimed to analyse the soil moisture variability and impacts on the agricultural production in the Bolivian Altiplano. For the soil moisture estimation with soil water balance, the most important input was precipitation and the outputs were runoff, percolation, and evapotranspiration. The remaining water was considered to be water stored in the soil. On the other hand, the estimations derived from satellite data were defined by assuming that the satellite data represent the soil moisture at the surface soil layer.

And, the soil moisture for deeper layers were defined by incorporating percolation and evapotranspiration interactions. Also here, the remaining water was considered to be stored soil moisture. The soil moisture estimations were related to quinoa yield for the identification of dry spell impact on agriculture. The findings can provide insights to improve the agricultural water management assist in sustainable management of water resources and drought risk reduction.

The drought risk in the Bolivian Altiplano was developed based on precipitation and temperature relationship with quinoa and potato yield during normal/moderate and El Niño (warm ENSO phase) years. A constraint for the analysis was the uneven and scarce distribution of ground data. Due to these limitations, we tested the performance of precipitation and temperature satellite imagery data. After proving that performance of the satellite data was satisfactory, precipitation and temperature variables were associated with the Normalized Difference Vegetation Index (NDVI). The NDVI data were used to simulate crop yield during the growing season. The findings show a significant decrease in crop yield during warm phase ENSO (El Niño years). With this information, we identified land areas where agricultural losses are most pronounced. Additionally, we found that precipitation and temperature explain most of the variance of crop production in the Bolivian Altiplano. Lower association is shown in the southern Altiplano where other variables might have larger influence. We found that during El Niño years the crop yield reduces considerably, and as a consequence the socio-economic vulnerability of farmers, will likely increase during such periods. Furthermore, it was found that NDVI can be related to crop yield and therefore, NDVI can be used to target specific hot spots depending on NDVI availability at a local scale. As a consequence, ENSO forecasts as well as possible magnitudes of crop deficits can be established that may be beneficial for emergency authorities, including identification of possible hotspots of crop deficits during the growing season. Our approach can help to determine the magnitude of assistance needed for farmers at the local level but also enable a proactive approach to disaster risk management against droughts. This may include not only economic related instruments such as insurance policy but also risk reduction instruments such as irrigation and resistant crop varieties as discussed above. In fact, risk based financing is gaining increasing attraction in real-world settings as it has several advantages. However, it should be acknowledged that large challenges still remain (French and Mechler, 2017).

This study aimed to assess the water scarcity in the Bolivian Altiplano. For this purpose, the precipitation anomalies, soil moisture variability and drought risk were analysed. Our study provided valuable information for climate forecasting and drought risk reduction. The precipitation variability in relation with climate phenomena could help to improve weather forecasting. Besides, identification of hotspots where crop yield is more affected by droughts, can improve drought risk management and provide information for the implementation of mitigation

strategies. The soil moisture estimations can improve agricultural and risk-based models. With such information, risk management plans can be set up with better accuracy. The findings enhance the knowledge for a sustainable water management, and drought disaster risk management in the Bolivian Altiplano.

References

- Aceituno, P. (1988). On the Functioning of the Southern Oscillation in the South American Sector. Part I: Surface Climate. *Monthly Weather Review*, 116(3), 505-524. doi:10.1175/1520-0493(1988)116<0505:OTFOTS>2.0.CO;2
- Allen, R. G., Pereira, L. S., Dirks, R., and Martin, S. (1998). *Crop evapotranspiration : Guidelines for computing crop water requirements*. Rome: Food and Agriculture Organization of the United Nations.
- Andreoli, R. V., and Kayano, M. T. (2005). ENSO-related rainfall anomalies in South America and associated circulation features during warm and cold Pacific decadal oscillation regimes. *International Journal of Climatology*, 25(15), 2017-2030. doi:10.1002/joc.1222
- Ayers, R. S., and Westcot, D. W. (1976). *Water quality for agriculture*. Rome: Food and Agriculture Organization of the United Nations.
- Baker, P. A., Rigsby, C. A., Seltzer, G. O., Fritz, S. C., Lowenstein, T. K., Bacher, N. P., and Veliz, C. (2001). Tropical climate changes at millennial and orbital timescales on the Bolivian Altiplano. *Nature*, 409(6821), 698-701. doi:10.1038/35055524
- Bartholmes, J. C., Thielen, J., Ramos, M. H., and Gentilini, S. (2009). The european flood alert system EFAS – Part 2: Statistical skill assessment of probabilistic and deterministic operational forecasts. *Hydrology and Earth System Sciences*, 13(2), 141-153. doi:10.5194/hess-13-141-2009
- Beck, P. S. A., Atzberger, C., Høgda, K. A., Johansen, B., and Skidmore, A. K. (2006). Improved monitoring of vegetation dynamics at very high latitudes: A new method using MODIS NDVI. *Remote Sensing of Environment*, 100(3), 321-334. doi:10.1016/j.rse.2005.10.021
- BID. (2016). Analisis ambiental y social *Programa de Saneamiento del Lago Titicaca*. La Paz, Bolivia: Banco Interamericano de Desarrollo (BID).
- Blacutt, L. A., Herdies, D. L., de Gonçalves, L. G. G., Vila, D. A., and Andrade, M. (2015). Precipitation comparison for the CFSR, MERRA, TRMM3B42 and Combined Scheme datasets in Bolivia. *Atmospheric Research*, 163(Supplement C), 117-131. doi:10.1016/j.atmosres.2015.02.002
- Botterill, L. E. C., and Fisher, M. (2003). *Beyond drought in Australia: people, policy and perspectives*. Collingwood., Victoria: CSIRO Publishing.
- Bretherton, C. S., Smith, C., and Wallace, J. M. (1992). An Intercomparison of Methods for Finding Coupled Patterns in Climate Data. *Journal of Climate*, 5(6), 541-560. doi:10.1175/1520-0442(1992)005<0541:aiomff>2.0.co;2

- Buxton, N., Escobar, M., Purkey, D., and Lima, N. (2013). *Water scarcity, climate change and Bolivia: Planning for climate uncertainties*. Davis, USA: Stockholm Environment Institute.
- Buytaert, W., and De Bièvre, B. (2012). Water for cities: The impact of climate change and demographic growth in the tropical Andes. *Water Resources Research*, 48(8). doi:10.1029/2011WR011755
- CAF. (2000). *Las lecciones de El Niño, Bolivia. Memorias del fenómeno El Niño 1997-1998, retos y propuestas para la región andina*. (Vol. II). Caracas, Venezuela: Corporación Andina de Fomento (CAF).
- Canedo-Rosso, C., Hochrainer-Stigler, S., Pflug, G., Condori, B., and Berndtsson, R. (2019a). Drought risk in the Bolivian Altiplano associated with El Niño Southern Oscillation using satellite imagery data. *Natural Hazards and Earth System Sciences Discussion*, 2019, 1-21. doi:10.5194/nhess-2018-403
- Canedo-Rosso, C., Uvo, C. B., and Berndtsson, R. (2019b). Precipitation variability and its relation to climate anomalies in the Bolivian Altiplano. *International Journal of Climatology*, 39(4), 2096-2107. doi:10.1002/joc.5937
- Canedo, C., Pillco Zolá, R., and Berndtsson, R. (2016). Role of Hydrological Studies for the Development of the TDPS System. *Water*, 8(4), 144. doi:10.3390/w8040144
- Chiang, J. C. H., and Vimont, D. J. (2004). Analogous Pacific and Atlantic Meridional Modes of Tropical Atmosphere–Ocean Variability. *Journal of Climate*, 17(21), 4143-4158. doi:10.1175/jcli4953.1
- Chuai, X. W., Huang, X. J., Wang, W. J., and Bao, G. (2013). NDVI, temperature and precipitation changes and their relationships with different vegetation types during 1998–2007 in Inner Mongolia, China. *International Journal of Climatology*, 33(7), 1696-1706. doi:10.1002/joc.3543
- CMLT. (2014). *Estado de la calidad ambiental de la Cuenca del Lago Titicaca ámbito Peruano*. Retrieved from Puno, Peru:
- Condom, T., Rau, P., and Espinoza, J. C. (2011). Correction of TRMM 3B43 monthly precipitation data over the mountainous areas of Peru during the period 1998–2007. *Hydrological Processes*, 25(12), 1924-1933. doi:10.1002/hyp.7949
- Condori, B., Hijmans, R., Ledent, J., and Quiroz, R. (2014). Managing Potato Biodiversity to Cope with Frost Risk in the High Andes: A Modeling Perspective. *PLoS ONE*, 9(1), e81510. doi:10.1371/journal.pone.0081510
- Cui, L., and Shi, J. (2010). Temporal and spatial response of vegetation NDVI to temperature and precipitation in eastern China. *Journal of Geographical Sciences*, 20(2), 163-176. doi:10.1007/s11442-010-0163-4
- Duan, Y., Wilson, A. M., and Barros, A. P. (2015). Scoping a field experiment: error diagnostics of TRMM precipitation radar estimates in complex terrain as a basis for IPHEX2014. *Hydrology and Earth System Sciences*, 19(3), 1501-1520. doi:10.5194/hess-19-1501-2015
- Enfield, D. B., Mestas-Nuñez, A. M., and Trimble, P. J. (2001). The Atlantic Multidecadal Oscillation and its relation to rainfall and river flows in the continental U.S. *Geophysical Research Letters*, 28(10), 2077-2080. doi:10.1029/2000GL012745

- Erickson, C. (1988). Raised field agriculture in the Lake Titicaca basi: Putting ancient agriculture back to work. *Expedition*, 30(1), 8-16.
- Feliks, Y., Ghil, M., and Robertson, A. W. (2010). Oscillatory climate modes in the Eastern Mediterranean and their synchronization with the North Atlantic Oscillation. *Journal of Climate*, 23(15), 4060-4079. doi:10.1175/2010jcli3181.1
- Flantua, S. G. A., Hooghiemstra, H., Vuille, M., Behling, H., Carson, J. F., Gosling, W. D., Hoyos, I., Ledru, M. P., Montoya, E., Mayle, F., Maldonado, A., Rull, V., Tonello, M. S., Whitney, B. S., and González-Arango, C. (2016). Climate variability and human impact in South America during the last 2000 years: synthesis and perspectives from pollen records. *Climate of the Past*, 12(2), 483-523. doi:10.5194/cp-12-483-2016
- French, A., and Mechler, R. (2017). *Managing El Niño Risks Under Uncertainty in Peru: Learning from the past for a more disaster-resilient future*. Retrieved from Laxenburg, Austria:
- Funk, C., Peterson, P., Landsfeld, M., Pedreros, D., Verdin, J., Shukla, S., Husak, G., Rowland, J., Harrison, L., Hoell, A., and Michaelsen, J. (2015). The climate hazards infrared precipitation with stations—a new environmental record for monitoring extremes. *A Nature Research Journal*, 2, 150066. doi:10.1038/sdata.2015.66
- Gámiz-Fortis, S. R., Pozo-Vázquez, D., Esteban-Parra, M. J., and Castro-Diez, Y. (2002). Spectral characteristics and predictability of the NAO assessed through Singular Spectral Analysis. *Journal of Geophysical Research: Atmospheres*, 107(D23), ACL 11-11-ACL 11-15. doi:10.1029/2001JD001436
- Garcia, M. (2003). *Agroclimatic Study and Drought Resistance Analysis of Quinoa for an Irrigation Strategy in the Bolivian Altiplano*: Katholieke Universiteit Leuven.
- Garcia, M., Raes, D., and Jacobsen, S.-E. (2003). Evapotranspiration analysis and irrigation requirements of quinoa (*Chenopodium quinoa*) in the Bolivian highlands. *Agricultural Water Management*, 60(2), 119-134. doi:10.1016/S0378-3774(02)00162-2
- Garcia, M., Raes, D., Jacobsen, S. E., and Michel, T. (2007). Agroclimatic constraints for rainfed agriculture in the Bolivian Altiplano. *Journal of Arid Environments*, 71(1), 109-121. doi:10.1016/j.jaridenv.2007.02.005
- Garreaud, R., Vuille, M., and Clement, A. C. (2003). The climate of the Altiplano: observed current conditions and mechanisms of past changes. *Palaeogeography, Palaeoclimatology, Palaeoecology*, 194(1-3), 5-22. doi:10.1016/S0031-0182(03)00269-4
- Garreaud, R. D. (2000). Intraseasonal variability of moisture and rainfall over the South American Altiplano. *Monthly Weather Review*, 128(9), 3337-3346. doi:10.1175/1520-0493(2000)128<3337:Ivomar>2.0.Co;2
- Garreaud, R. D. (2009). The Andes climate and weather. *Advances in geosciences*, 22, 3-11. doi:10.5194/adgeo-22-3-2009
- Garreaud, R. D., and Aceituno, P. (2001). Interannual rainfall variability over the South American Altiplano. *Journal of Climate*, 14(12), 2779-2789. doi:10.1175/1520-0442(2001)014<2779:Irvots>2.0.Co;2

- Garreaud, R. D., Vuille, M., Compagnucci, R., and Marengo, J. (2009). Present-day South American climate. *Palaeogeography, Palaeoclimatology, Palaeoecology*, 281(3-4), 180-195. doi:10.1016/j.palaeo.2007.10.032
- Geerts, S., Raes, D., Garcia, M., Del Castillo, C., and Buytaert, W. (2006). Agro-climatic suitability mapping for crop production in the Bolivian Altiplano: A case study for quinoa. *Agricultural and Forest Meteorology*, 139(3), 399-412. doi:10.1016/j.agrformet.2006.08.018
- Geerts, S., Raes, D., Garcia, M., Mendoza, J., and Huanca, R. (2008a). Crop water use indicators to quantify the flexible phenology of quinoa (*Chenopodium quinoa* Willd.) in response to drought stress. *Field Crops Research*, 108(2), 150-156. doi:10.1016/j.fcr.2008.04.008
- Geerts, S., Raes, D., Garcia, M., Miranda, R., Cusicanqui, J. A., Taboada, C., Mendoza, J., Huanca, R., Mamani, A., Condori, O., Mamani, J., Morales, B., Osco, V., and Steduto, P. (2009). Simulating Yield Response of Quinoa to Water Availability with AquaCrop. *Agronomy Journal*, 101(3), 499-508. doi:10.2134/agronj2008.0137s
- Geerts, S., Raes, D., Garcia, M., Vacher, J., Mamani, R., Mendoza, J., Huanca, R., Morales, B., Miranda, R., Cusicanqui, J., and Taboada, C. (2008b). Introducing deficit irrigation to stabilize yields of quinoa (*Chenopodium quinoa* Willd.). *European Journal of Agronomy*, 28(3), 427-436. doi:10.1016/j.eja.2007.11.008
- Goupillaud, P., Grossmann, A., and Morlet, J. (1984). Cycle-octave and related transforms in seismic signal analysis. *Geoexploration*, 23(1), 85-102. doi:10.1016/0016-7142(84)90025-5
- Grinsted, A., Moore, J. C., and Jevrejeva, S. (2004). Application of the cross wavelet transform and wavelet coherence to geophysical time series. *Nonlinear Processes in Geophysics*, 11(5/6), 561-566. doi:10.5194/npg-11-561-2004
- Grossmann, A., and Morlet, J. (1984). Decomposition of Hardy Functions into Square Integrable Wavelets of Constant Shape. *SIAM Journal on Mathematical Analysis*, 15(4), 723-736. doi:10.1137/0515056
- Grossmann, I., and Klotzbach, P. J. (2009). A review of North Atlantic modes of natural variability and their driving mechanisms. *Journal of Geophysical Research: Atmospheres*, 114(D24107), n.a.-n.a. doi:10.1029/2009JD012728
- Guha-Sapir, D., Hoyois, P., Wallemacq, P., and Below, R. (2016). *Annual Disaster Statistical Review 2016: The numbers and trends*. Retrieved from Brussels: emdat.be/sites/default/files/adsr_2016.pdf
- Hagman, G., Beer, H., and Svenska röda, k. (1984). *Prevention better than cure: report on human and environmental disasters in the Third World*. Stockholm: Swedish Red Cross.
- Heim, R. R. (2002). A Review of Twentieth-Century Drought Indices Used in the United States. *Bulletin of the American Meteorological Society*, 83(8), 1149-1166. doi:10.1175/1520-0477-83.8.1149
- Holben, B. N. (1986). Characteristics of maximum-value composite images from temporal AVHRR data. *International Journal of Remote Sensing*, 7(11), 1417-1434. doi:10.1080/01431168608948945

- Hotelling, H. (1933). Analysis of a complex of statistical variables into principal components. *Journal of Educational Psychology*, 24(6), 417-441. doi:10.1037/h0071325
- Huang, J., Higuchi, K., and Shabbar, A. (1998). The relationship between the North Atlantic Oscillation and El Niño-Southern Oscillation. *Geophysical Research Letters*, 25(14), 2707-2710. doi:10.1029/98GL01936
- Huang, J., Wang, H., Dai, Q., and Han, D. (2014a). Analysis of NDVI Data for Crop Identification and Yield Estimation. *IEEE Journal of Selected Topics in Applied Earth Observations and Remote Sensing*, 7(11), 4374-4384. doi:10.1109/JSTARS.2014.2334332
- Huang, Y., Liu, X., Shen, Y., and Jin, J. (2014b, 11-14 Aug. 2014). *Assessment of agricultural drought indicators impact on soybean crop yield: A case study in Iowa, USA*. Paper presented at the 2014 The Third International Conference on Agro-Geoinformatics.
- Hunziker, S., Brönnimann, S., Calle, J., Moreno, I., Andrade, M., Ticona, L., Huerta, A., and Lavado-Casimiro, W. (2018). Effects of undetected data quality issues on climatological analyses. *Climate of the Past*, 14(1), 1-20. doi:10.5194/cp-14-1-2018
- INE. (2015a). *Censo Agropecuario de Bolivia 2013* (first ed. Vol. 2016). La Paz: The National Institute of Statistics (INE) of Bolivia.
- INE. (2015b). *Censo de Población y Vivienda Bolivia 2012: Características de la Población* (first ed.). La Paz: The National Institute of Statistics (INE) of Bolivia.
- IPCC. (2013). *Climate Change 2013: The Physical Science Basis. Contribution of Working Group I to the Fifth Assessment Report of the Intergovernmental Panel on Climate Change* (T. F. Stocker, D. Qin, G.-K. Plattner, M. Tignor, S. K. Allen, J. Boschung, A. Nauels, Y. Xia, V. Bex, and G. F. Midgley Eds.). Cambridge, United Kingdom and New York, NY, USA: Cambridge University Press.
- Jacobsen, S. E., and Bach, A. P. (1998). The influence of temperature on seed germination rate in quinoa (*Chenopodium quinoa* Willd. *Seed Science and Technology (Switzerland)*, 26(2), 515-523.
- Jacobsen, S. E., Monteros, C., Christiansen, J. L., Bravo, L. A., Corcuera, L. J., and Mujica, A. (2005). Plant responses of quinoa (*Chenopodium quinoa* Willd.) to frost at various phenological stages. *European Journal of Agronomy*, 22(2), 131-139. doi:10.1016/j.eja.2004.01.003
- Jacobsen, S. E., Mujica, A., and Jensen, C. R. (2003). The resistance of quinoa (*Chenopodium quinoa* Willd.) to adverse abiotic factors. *Food Reviews International*, 19(1-2), 99-109. doi:10.1081/FRI-120018872
- Ji, L., and Peters, A. J. (2003). Assessing vegetation response to drought in the northern Great Plains using vegetation and drought indices. *Remote Sensing of Environment*, 87(1), 85-98. doi:10.1016/S0034-4257(03)00174-3
- Jones, P. D., Jonsson, T., and Wheeler, D. (1997). Extension to the North Atlantic oscillation using early instrumental pressure observations from Gibraltar and south-west Iceland. *International Journal of Climatology*, 17(13), 1433-1450. doi:10.1002/(SICI)1097-0088(19971115)17:13<1433::AID-JOC203>3.0.CO;2-P

- Kayano, M. T., and Andreoli, R. V. (2007). Relations of South American summer rainfall interannual variations with the Pacific Decadal Oscillation. *International Journal of Climatology*, 27(4), 531-540. doi:10.1002/joc.1417
- Kerr, R. A. (2000). A North Atlantic climate pacemaker for the centuries. *Science*, 288(5473), 1984-1985. doi:10.1126/science.288.5473.1984
- Knight, J. R., Allan, R. J., Folland, C. K., Vellinga, M., and Mann, M. E. (2005). A signature of persistent natural thermohaline circulation cycles in observed climate. *Geophysical Research Letters*, 32(20). doi:10.1029/2005GL024233
- Kossin, J. P., Camargo, S. J., and Sitkowski, M. (2010). Climate modulation of North Atlantic hurricane tracks. *Journal of Climate*, 23(11), 3057-3076. doi:10.1175/2010jcli3497.1
- Kossin, J. P., and Vimont, D. J. (2007). A more general framework for understanding Atlantic hurricane variability and trends. *Bulletin of the American Meteorological Society*, 88(11), 1767-1782. doi:10.1175/bams-88-11-1767
- Kutner, M. H., Nachtsheim, C., and Neter, J. (2004). *Applied linear regression models*: McGraw-Hill/Irwin.
- Lal, P. N., Mitchell, T., Aldunce, P., Auld, H., Mechler, R., Miyani, A., Romano, L. E., and Zakaria, S. (2012). National systems for managing the risks from climate extremes and disasters In C. B. Field, V. Barros, T. F. Stocker, D. Qin, D. J. Dokken, K. L. Ebi, M. D. Mastrandrea, K. J. Mach, G.-K. Plattner, S. K. Allen, M. Tignor, and P. M. Midgley (Eds.), *Managing the Risks of Extreme Events and Disasters to Advance Climate Change Adaptation: A Special Report of Working Groups I and II of the Intergovernmental Panel on Climate Change (IPCC)* (pp. 339-392). Cambridge University Press, Cambridge, UK, and New York, NY, USA.
- Lenters, J. D., and Cook, K. H. (1997). On the origin of the Bolivian High and related circulation features of the South American climate. *Journal of the Atmospheric Sciences*, 54(5), 656-678. doi:10.1175/1520-0469(1997)054<0656:OTOOTB>2.0.CO;2
- Lenters, J. D., and Cook, K. H. (1999). Summertime precipitation variability over South America: Role of the large-scale circulation. *Monthly Weather Review*, 127(3), 409-431. doi:10.1175/1520-0493(1999)127<0409:Spvosa>2.0.Co;2
- Li, Y., and Lau, N.-C. (2012). Impact of ENSO on the atmospheric variability over the North Atlantic in late winter-role of transient eddies. *Journal of Climate*, 25(1), 320-342. doi:10.1175/jcli-d-11-00037.1
- Mächel, H., Kapala, A., and Flohn, H. (1998). Behaviour of the centres of action above the Atlantic since 1881. Part I: Characteristics of seasonal and interannual variability. *International Journal of Climatology*, 18(1), 1-22. doi:10.1002/(SICI)1097-0088(199801)18:1<1::AID-JOC225>3.0.CO;2-A
- Mantua, N. J., and Hare, S. R. (2002). The Pacific Decadal Oscillation. *Journal of Oceanography*, 58(1), 35-44. doi:10.1023/a:1015820616384
- Mantua, N. J., Hare, S. R., Zhang, Y., Wallace, J. M., and Francis, R. C. (1997). A Pacific Interdecadal Climate Oscillation with Impacts on Salmon Production. *Bulletin of the*

- American Meteorological Society*, 78(6), 1069-1079. doi:10.1175/1520-0477(1997)078<1069:apicow>2.0.co;2
- Marengo, J. A., Espinoza, J. C., Alves, L. M., and Ronchail, J. (2017). Drought in Bolivia: The worst in the last 25 years. In J. Blunden and D. S. Arndt (Eds.), *State of Climate in 2016* (Vol. 98, pp. S188-S189): Bulletin of the American Meteorological Society.
- Marshall, J., Kushnir, Y., Battisti, D., Chang, P., Czaja, A., Dickson, R., Hurrell, J., McCartney, M., Saravanan, R., and Visbeck, M. (2001). North Atlantic climate variability: phenomena, impacts and mechanisms. *International Journal of Climatology*, 21(15), 1863-1898. doi:10.1002/joc.693
- McKee, T. B., Doesken, N. J., and Kleist, J. (1993). *The Relationship of Drought Frequency and Duration to Time Scales*. Paper presented at the 8th Conference on Applied Climatology, Anaheim.
- Mills, C. M., and Walsh, J. E. (2013). Seasonal Variation and Spatial Patterns of the Atmospheric Component of the Pacific Decadal Oscillation. *Journal of Climate*, 26(5), 1575-1594. doi:10.1175/jcli-d-12-00264.1
- Minobe, S. (1999). Resonance in bidecadal and pentadecadal climate oscillations over the North Pacific: Role in climatic regime shifts. *Geophysical Research Letters*, 26(7), 855-858. doi:10.1029/1999GL900119
- Mishra, A. K., and Singh, V. P. (2010). A review of drought concepts. *Journal of Hydrology*, 391(1), 202-216. doi:10.1016/j.jhydrol.2010.07.012
- MMAyA. (2010). *Plan director de la cuenca Katari*. La Paz, Bolivia.
- Morales, M. S., Christie, D. A., Villalba, R., Argollo, J., Pacajes, J., Silva, J. S., Alvarez, C. A., Llanabure, J. C., and Soliz Gamboa, C. C. (2012). Precipitation changes in the South American Altiplano since 1300 AD reconstructed by tree-rings. *Climate of the Past*, 8(2), 653-666. doi:10.5194/cp-8-653-2012
- Moriasi, D. N., Arnold, J. G., Van Liew, M. W., Bingner, R. L., Harmel, R. D., and Veith, T. L. (2007). Model Evaluation Guidelines for Systematic Quantification of Accuracy in Watershed Simulations. *Transactions of the ASABE*, 50(3), 885-900. doi:10.13031/2013.23153
- Morlet, J. (1983). Sampling Theory and Wave Propagation. In C. H. Chen (Ed.), *Issues in Acoustic Signal — Image Processing and Recognition* (Vol. 1, pp. 233-261). Berlin, Heidelberg: Springer.
- Nash, J. E., and Sutcliffe, J. V. (1970). River flow forecasting through conceptual models part I — A discussion of principles. *Journal of Hydrology*, 10(3), 282-290. doi:10.1016/0022-1694(70)90255-6
- Null, J. (2018). El Niño and La Niña Years and Intensities. Retrieved from <https://ggweather.com/enso/oni.htm>
- Ochoa, A., Pineda, L., Crespo, P., and Willems, P. (2014). Evaluation of TRMM 3B42 precipitation estimates and WRF retrospective precipitation simulation over the Pacific–Andean region of Ecuador and Peru. *Hydrology and Earth System Sciences*, 18(8), 3179-3193. doi:10.5194/hess-18-3179-2014

- Ormachea, E., and Ramirez, N. (2013). *Propiedad colectiva de la tierra y producción agrícola capitalista: El caso de la quinua en el Altiplano Sur de Bolivia* (first ed.). Bolivia: Centro de Estudios para el Desarrollo Laboral y Agrario (CEDLA).
- Paluš, M., and Novotná, D. (2011). Northern Hemisphere patterns of phase coherence between solar/geomagnetic activity and NCEP/NCAR and ERA40 near-surface air temperature in period 7–8 years oscillatory modes. *Nonlinear Processes in Geophysics*, 18(2), 251-260. doi:10.5194/npg-18-251-2011
- Pearson, K. (1901). On lines and planes of closest fit to systems of points in space. *Philosophical Magazine*, 2(11), 559-572. doi:10.1080/14786440109462720
- Penman, H. L. (1948). Natural evaporation from open water, bare soil and grass. *Proceedings of the Royal Society of London. Series A. Mathematical and Physical Sciences*, 193(1032), 120-145. doi:10.1098/rspa.1948.0037
- Pillco, R., and Bengtsson, L. (2006). Long-term and extreme water level variations of the shallow Lake Poopó, Bolivia. *Hydrological Sciences Journal*, 51(1), 98-114. doi:10.1623/hysj.51.1.98
- Rana, A., Uvo, C. B., Bengtsson, L., and Parth Sarthi, P. (2012). Trend analysis for rainfall in Delhi and Mumbai, India. *Climate Dynamics*, 38(1), 45-56. doi:10.1007/s00382-011-1083-4
- Rayner, N. A., Parker, D. E., Horton, E. B., Folland, C. K., Alexander, L. V., Rowell, D. P., Kent, E. C., and Kaplan, A. (2003). Global analyses of sea surface temperature, sea ice, and night marine air temperature since the late nineteenth century. *Journal of Geophysical Research: Atmospheres*, 108(D14), n/a-n/a. doi:10.1029/2002JD002670
- Rencher, A. C. (1995). *Methods of Multivariate Analysis*. New York: John Wiley & Sons.
- Repo-Carrasco-Valencia, R. A.-M., and Serna, L. A. (2011). Quinoa (*Chenopodium quinoa*, Willd.) as a source of dietary fiber and other functional components. *Food Science and Technology*, 31(1), 225-230. doi:10.1590/S0101-20612011000100035
- Revollo, M. M. (2001). Management issues in the Lake Titicaca and Lake Poopo system: Importance of developing a water budget. *Lakes & Reservoirs: Research and Management*, 6(3), 225-229. doi:10.1046/j.1440-1770.2001.00151.x
- Richerson, P. J., Widmer, C., and Kittel, T. (1977). *The limnology of Lake Titicaca (Peru-Bolivia): a large, high altitude tropical lake*. Davis, Calif.: Institute of Ecology, University of California.
- Rivière, G., and Drouard, M. (2015). Understanding the contrasting North Atlantic Oscillation anomalies of the winters of 2010 and 2014. *Geophysical Research Letters*, 42(16), 6868-6875. doi:10.1002/2015GL065493
- Rogers, J. C. (1984). The Association between the North Atlantic Oscillation and the Southern Oscillation in the Northern Hemisphere. *Monthly Weather Review*, 112(10), 1999-2015. doi:10.1175/1520-0493(1984)112<1999:tabtna>2.0.co;2
- Ronchail, J., and Gallaire, R. (2006). ENSO and rainfall along the Zongo valley (Bolivia) from the Altiplano to the Amazon basin. *International Journal of Climatology*, 26(9), 1223-1236. doi:10.1002/joc.1296

- Sandford, S. (1979). *Towards a definition of drought*. Paper presented at the Botswana Drought Symposium, Gaborone, Botswana.
- Santos, J. L. (2006). The Impact of El Niño - Southern Oscillation Events on South America. *Advances in geosciences*, 6, 221-225. doi:10.5194/adgeo-6-221-2006
- Satgé, F., Bonnet, M.-P., Gosset, M., Molina, J., Hernan Yuque Lima, W., Pillco Zolá, R., Timouk, F., and Garnier, J. (2016). Assessment of satellite rainfall products over the Andean plateau. *Atmospheric Research*, 167, 1-14. doi:10.1016/j.atmosres.2015.07.012
- Satgé, F., Espinoza, R., Zolá, R. P., Roig, H., Timouk, F., Molina, J., Garnier, J., Calmant, S., Seyler, F., and Bonnet, M.-P. (2017). Role of Climate Variability and Human Activity on Poopó Lake Droughts between 1990 and 2015 Assessed Using Remote Sensing Data. *Remote Sensing*, 9(3), 218. doi:10.3390/rs9030218
- Savabi, M. R., and Williams, J. R. (1995). Chapter 5. Water balance and percolation. In D. C. Flanagan, M. A. Nearing, and J. M. Laflen (Eds.), *Water Erosion Prediction Project: Hillslope Profile and Watershed Model Documentation* (Vol. NSERL Report No. 10). West Lafayette, US: USDA-ARS National Soil Erosion Research Laboratory.
- Saxton, K. E., and Rawls, W. J. (2006). Soil Water Characteristic Estimates by Texture and Organic Matter for Hydrologic Solutions. *Soil Science Society of America Journal*, 70(5), 1569-1578. doi:10.2136/sssaj2005.0117
- Schlesinger, M. E., and Ramankutty, N. (1994). An oscillation in the global climate system of period 65–70 years. *Nature*, 367, 723-726. doi:10.1038/367723a0
- Sen, A. K., and Ogrin, D. (2016). Analysis of monthly, winter, and annual temperatures in Zagreb, Croatia, from 1864 to 2010: the 7.7-year cycle and the North Atlantic Oscillation. *Theoretical and Applied Climatology*, 123(3), 733-739. doi:10.1007/s00704-015-1388-z
- Shinoda, M. (1995). Seasonal phase lag between rainfall and vegetation activity in tropical Africa as revealed by NOAA satellite data. *International Journal of Climatology*, 15(6), 639-656. doi:10.1002/joc.3370150605
- Shrestha, N. K., Qamer, F. M., Pedreros, D., Murthy, M. S. R., Wahid, S. M., and Shrestha, M. (2017). Evaluating the accuracy of Climate Hazard Group (CHG) satellite rainfall estimates for precipitation based drought monitoring in Koshi basin, Nepal. *Journal of Hydrology: Regional Studies*, 13, 138-151. doi:10.1016/j.ejrh.2017.08.004
- Shukla, S., Steinemann, A., Iacobellis, S. F., and Cayan, D. R. (2015). Annual drought in California: association with monthly precipitation and climate phases. *Journal of Applied Meteorology and Climatology*, 54(11), 2273-2281. doi:10.1175/jamc-d-15-0167.1
- Smakhtin, V. U. (2001). Low flow hydrology: a review. *Journal of Hydrology*, 240(3), 147-186. doi:10.1016/S0022-1694(00)00340-1
- Smirnov, D., and Vimont, D. J. (2011). Variability of the Atlantic Meridional Mode during the Atlantic hurricane season. *Journal of Climate*, 24(5), 1409-1424. doi:10.1175/2010jcli3549.1

- Spinoni, J., Naumann, G., Carrao, H., Barbosa, P., and Vogt, J. (2014). World drought frequency, duration, and severity for 1951–2010. *International Journal of Climatology*, 34(8), 2792-2804. doi:10.1002/joc.3875
- Sun, Y., Liu, F., Bendevis, M., Shabala, S., and Jacobsen, S.-E. (2014). Sensitivity of two quinoa (*Chenopodium quinoa* Willd.) varieties to progressive drought stress. *Journal of Agronomy and Crop Science*, 200(1), 12-23. doi:10.1111/jac.12042
- Talebnejad, R., and Sepaskhah, A. R. (2015). Effect of deficit irrigation and different saline groundwater depths on yield and water productivity of quinoa. *Agricultural Water Management*, 159, 225-238. doi:10.1016/j.agwat.2015.06.005
- Thibeault, J., Seth, A., and Wang, G. L. (2012). Mechanisms of summertime precipitation variability in the Bolivian Altiplano: present and future. *International Journal of Climatology*, 32(13), 2033-2041. doi:10.1002/joc.2424
- Thompson, L. G., Mosley-Thompson, E., and Arnao, B. M. (1984). El Niño-Southern Oscillation events recorded in the stratigraphy of the tropical Quelccaya ice cap, Peru. *Science*, 226(4670), 50-53. doi:10.1126/science.226.4670.50
- Torrence, C., and Compo, G. P. (1998). A Practical Guide to Wavelet Analysis. *Bulletin of the American Meteorological Society*, 79(1), 61-78. doi:10.1175/1520-0477(1998)079<0061:apgtwa>2.0.co;2
- Torrence, C., and Webster, P. J. (1999). Interdecadal Changes in the ENSO–Monsoon System. *Journal of Climate*, 12(8), 2679-2690. doi:10.1175/1520-0442(1999)012<2679:icitem>2.0.co;2
- UN. (2015). *Sendai Framework for Disaster Risk Reduction 2015-2030*. Retrieved from Geneva, Switzerland:
- UN. (2016). *The Sustainable Development Goals Report 2016*. New York, USA: United Nations
- UNDP. (2011). *Tras las huellas del cambio climático en Bolivia. Estado del arte del conocimiento sobre adaptación al cambio climático: agua y seguridad alimentaria*. La Paz, Bolivia: UNDP-Bolivia.
- UNEP. (1996). *Diagnostico Ambiental del Sistema Titicaca-Desaguadero-Poopo-Salar de Coipasa (Sistema TDPS) Bolivia-Perú*. Retrieved from Washington, D.C.:
- UNESCO-WWAP. (2003). *Water for people, water for life* (Vol. 1). Paris/New York: UNESCO and Berghahn Books.
- UNISDR. (2009). *Drought Risk Reduction Framework and Practices: Contributing to the Implementation of the Hyogo Framework for Action*. Geneva, Switzerland: United Nations secretariat of the International Strategy for Disaster Reduction (UNISDR).
- UNISDR. (2015). *Making Development Sustainable: The Future of Disaster Risk Management. Global Assessment Report on Disaster Risk Reduction*. Retrieved from Geneva, Switzerland:
- Uvo, C. B., Repelli, C. A., Zebiak, C., and Kushnir, Y. (1997). A study influence of the Pacific and Atlantic SST on the Northeast Brazil monthly precipitation using singular value decomposition. In F. Garcia-Garcia, G. Cisneros, A. Fernández-Eguiarte, and R. Álvarez (Eds.), *Numerical Simulations in the Environmental and Earth Sciences*:

- Proceedings of the Second UNAM-CRAY Supercomputing Conference*. New York, NY, USA: Cambridge University Press.
- Verbist, K., Amani, A., Mishra, A., and Cisneros, B. J. (2016). Strengthening drought risk management and policy: UNESCO International Hydrological Programme's case studies from Africa and Latin America and the Caribbean. *Water Policy*, 18(S2), 245-261. doi:10.2166/wp.2016.223
- Vicente-Serrano, S. M., Chura, O., López-Moreno, J. I., Azorin-Molina, C., Sanchez-Lorenzo, A., Aguilar, E., Moran-Tejeda, E., Trujillo, F., Martínez, R., and Nieto, J. J. (2015). Spatio-temporal variability of droughts in Bolivia: 1955–2012. *International Journal of Climatology*, 35(10), 3024-3040. doi:10.1002/joc.4190
- Vimont, D. J., and Kossin, J. P. (2007). The Atlantic Meridional Mode and hurricane activity. *Geophysical Research Letters*, 34(7), n.a.-n.a. doi:10.1029/2007GL029683
- Vuille, M. (1999). Atmospheric circulation over the Bolivian Altiplano during dry and wet periods and extreme phases of the Southern Oscillation. *International Journal of Climatology*, 19(14), 1579-1600. doi:10.1002/(SICI)1097-0088(19991130)19:14<1579::AID-JOC441>3.0.CO;2-N
- Vuille, M., Bradley, R. S., and Keimig, F. (2000). Interannual climate variability in the Central Andes and its relation to tropical Pacific and Atlantic forcing. *Journal of Geophysical Research: Atmospheres*, 105(D10), 12447-12460. doi:10.1029/2000JD900134
- Vuille, M., and Keimig, F. (2004). Interannual variability of summertime convective cloudiness and precipitation in the Central Andes derived from ISCCP-B3 Data. *Journal of Climate*, 17(17), 3334-3348. doi:10.1175/1520-0442(2004)017<3334:IVOSCC>2.0.CO;2
- Walker, G. T., and Bliss, E. W. (1932). World Weather V. *Memoirs of the Royal Meteorological Society*, 4(36), 53-84.
- Wallace, J. M., Smith, C., and Bretherton, C. S. (1992). Singular Value Decomposition of Wintertime Sea Surface Temperature and 500-mb Height Anomalies. *Journal of Climate*, 5(6), 561-576. doi:10.1175/1520-0442(1992)005<0561:svdows>2.0.co;2
- Wilhite, D. A., and Glantz, M. H. (1985). Understanding: The Drought Phenomenon: The Role of Definitions. In D. A. Wilhite, W. E. Easterling, and D. A. Wood (Eds.), *Planning for Drought: Toward a Reduction of Social Vulnerability* (pp. 10-30). Boulder, USA: Westview Press.
- Wilks, D. S. (2006). *Statistical Methods in the Atmospheric Sciences* (second ed. Vol. 100): Academic Press.
- Winkel, T., Álvarez-Flores, R., Bommel, P., Bourliaud, J., Chevarría Lazo, M., Cortes, G., Cruz, P., Del Castillo, C., Gasselin, P., Joffre, R., Léger, F., Nina Laura, J. P., Rambal, S., Riviére, G., Tichit, M., Tourrand, J. F., Vassas Toral, A., and Vieira Pak M. (2015). The Southern Altiplano of Bolivia. In FAO and CIRAD (Eds.), *State of the Art Report of Quinoa in the World in 2013*. Rome.
- WMO. (2006). *Drought monitoring and early warning: concepts, progress and future challenges*. Geneva, Switzerland: World Meteorological Organization (WMO).

- World-Bank. (2009). *Bolivia - Country note on climate change aspects in agriculture*. (World-Bank Ed.). Washington, DC.
- Xie, S.-P., and Carton, J. A. (2004). Tropical Atlantic Variability: Patterns, Mechanisms, and Impacts. In C. Wang, S. Xie, and J. Carton (Eds.), *Earth's Climate* (pp. 121-142): American Geophysical Union.
- Yihdego, Y., Vaheddoost, B., and Al-Weshah, R. A. (2019). Drought indices and indicators revisited. *Arabian Journal of Geosciences*, 12(3), 69. doi:10.1007/s12517-019-4237-z
- Zhang, Y., Wallace, J. M., and Battisti, D. S. (1997). ENSO-like Interdecadal Variability: 1900–93. *Journal of Climate*, 10(5), 1004-1020. doi:10.1175/1520-0442(1997)010<1004:eliv>2.0.co;2
- Zhou, J., and Lau, K.-M. (1998). Does a monsoon climate exist over South America? *Journal of Climate*, 11(5), 1020-1040. doi:10.1175/1520-0442(1998)011<1020:dameo>2.0.co;2



This thesis is the compilation of an extraordinary journey that started with the question: Is there a path to improve the sustainability of local livelihood in the Bolivian highlands? In this arid region, available water is often insufficient to meet existing demand. Here, the agricultural sector is the most affected counting large production losses. Sustainable water management can reduce the water stress and drought impacts. However, drought preparedness requires a detailed comprehension of the problem. Thus, the main goal of this study was to address the Bolivian Altiplano water scarcity to develop sustainable water management. For this, variability of rainfall and soil moisture was evaluated. Along this line, agricultural drought was related to climatic observations. The findings of this study provide insights to identify strategies for improving water management in the Bolivian Altiplano, mainly during water stress conditions. Moreover, the results can enhance the knowledge regarding hydroclimatological variability in the Altiplano for drought disaster risk management, proactive planning, and mitigation policy measures in vulnerable regions.

